AD-A216 840

NAVAL POSTGRADUATE SCHOOL
Monterey, California

THESIS

PROCESSING AND ELEVATED TEMPERATURE DUCTILITY OF ALUMINUM ALLOY 7475

by

John Ratkovich

June 1989

Thesis Advisor Terry R. McNelley

Approved for public release; distribution is unlimited.

9 0 01 17 129

Unclassified

security classification of this page

REPORT DOCUMENTATION PAGE

1a Report Security Classification Unclassified	1b Restrictive Markings
2a Security Classification Authority	3 Distribution Availability of Report
2b Declassification Downgrading Schedule	Approved for public release; distribution is unlimited.
4 Performing Organization Report Number(s)	5 Monitoring Organization Report Number(s)
6a Name of Performing Organization: Naval Postgraduate School; 6b Office Symbol (if applicable): 52	7a Name of Monitoring Organization: Naval Postgraduate School
6c Address (city, state, and ZIP code): Monterey, CA 93943-5000	7b Address (city, state, and ZIP code): Monterey, CA 93943-5000
8a Name of Funding Sponsoring Organization; 8b Office Symbol (if applicable)	9 Procurement Instrument Identification Number
8c Address (city, state, and ZIP code)	10 Source of Funding Numbers: Program Element No; Project No; Task No; Work Unit Accession No

11 Title (include security classification) PROCESSING AND ELEVATED TEMPERATURE DUCTILITY OF ALUMINUM ALLOY 7475

12 Personal Author(s) John Ratkovich

13a Type of Report	13b Time Covered	14 Date of Report (year, month, day)	15 Page Count
Master's Thesis	From To	June 1989	59

16 Supplementary Notation The views expressed in this thesis are those of the author and do not reflect the official policy or position of the Department of Defense or the U.S. Government.

17 Cosati Codes			18 Subject Terms (continue on reverse if necessary and identify by block number)
Field	Group	Subgroup	Thermomechanical Processing, Superplasticity, Al 7475, Cavitation.

19 Abstract (continue on reverse if necessary and identify by block number)

This research has initiated investigation of Al alloy 7475 (Al-Zn-Mg-Cu) in regard to the effects of thermomechanical process (TMP) variables on superplasticity. These effects are evaluated by pct. elongation at temperatures ranging from 300-450°C and strain rates of 6.7×10^{-3} to 6.7×10^{-5} s^{-1} and microstructural analysis. In comparison to results in the literature, superplastic ductility for lower temperature, higher rate superplasticity may be enhanced.

20 Distribution Availability of Abstract	21 Abstract Security Classification	
☒ unclassified unlimited ☐ same as report ☐ DTIC users	Unclassified	
22a Name of Responsible Individual: Terry R. McNelley	22b Telephone (include Area code): (408) 646-2589	22c Office Symbol: 69Mc

DD FORM 1473,84 MAR 83 APR edition may be used until exhausted. All other editions are obsolete.

security classification of this page

Unclassified

Approved for public release; distribution is unlimited.

Processing and Elevated Temperature Ductility
of Aluminum Alloy 7475

by

John Ratkovich
Lieutenant, United States Navy
B.S.M.E., United States Naval Academy, 1982

Submitted in partial fulfillment of the
requirements for the degree of

MASTER OF SCIENCE IN MECHANICAL ENGINEERING

from the

NAVAL POSTGRADUATE SCHOOL
June 1989

Author: John Ratkovich
John Ratkovich

Approved by:
Terry R. McNelley, Thesis Advisor

Anthony J. Healey, Chairman,
Department of Mechanical Engineering

Gordon E. Schacher,
Dean of Science and Engineering

ABSTRACT

This research has initiated investigation of Al alloy 7475 (Al-Zn-Mg-Cu) in regard to the effects of thermomechanical process (TMP) variables on superplasticity. These effects are evaluated by pct. elongation at temperatures ranging from 300-450°C and strain rates of 6.7×10^{-3} to 6.7×10^{-5} s^{-1} and microstructural analysis. In comparison to results in the literature, superplastic ductility for lower temperature, higher rate superplasticity may be enhanced.

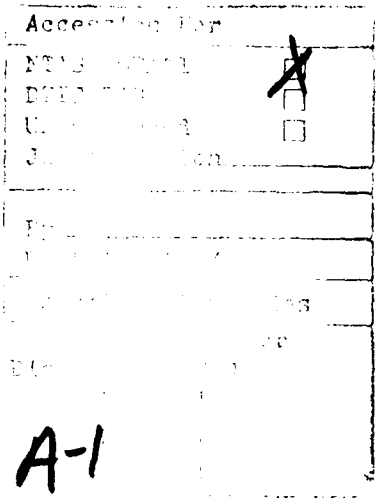

TABLE OF CONTENTS

LIST OF TABLES

LIST OF FIGURES

ACKNOWLEDGMENT

I thank Professor Terry McNelley for the professional guidance and incessant support he gave to me throughout this project. I thank my parents for their never ending interest and support of my 19 years of schooling. I thank my wife, Stacie, for her encouragement and support during our two year stay here in Monterey. I thank my children, Brian and Kylie, for their inspiration to learn and grow each and every day.

I. INTRODUCTION

The purpose of this project was to investigate the effects of thermomechanical processing (TMP) variables on the superplastic behavior (elongation>200%) of Aluminum (Al) alloy 7475 (Al-Zn-Mg-Cu). This project has focused on the commercially available wrought form of Al 7475 and not on specially melted or powder products.

The experimental work done in this project is an effort to apply a metallurgical model that has been proposed by Hales and McNelley [Ref. 1: p.72] to describe microstructural evolution during TMP that will promote superplasticity during subsequent tensile testing of the material. Thus, dislocations introduced during working of the material (by passing the material through the rolling mill) are allowed to recover by reheating the material between rolling passes. The recovery consists of the dislocations realigning themselves to form a substructure within the existing grain structure. A second effect of the heating is that precipitates form within the grain structure because the elevated temperature (below the solvus temperature) facilitates the diffusion necessary for precipitation. These precipitates serve the role of stabilizing the dislocation substructure so that it may transform into a refined grain structure through a cycle of rolling and annealing treatments. This refinement of the original grain structure essentially conditions the material to sustain superplastic deformation mechanisms.

The goal of the conditioning is to produce a refined structure of sufficiently misoriented boundaries to allow the sliding of the grains when the material is subsequently stressed. This sliding of the grains is the central feature of superplasticity. It has been determined for Al-Mg alloys that boundary misorientation in the range of 2-7° is sufficient [Ref. 1: p.72]. Misorientations less than this result in inhibited sliding while misorientations greater than this may result in grain boundary energy high enough to

promote grain growth, which in turn counteracts the necessity to retain a refined microstructure. The sliding phenomenon that leads to superplasticity requires accommodation of the sliding grains to occur. That is, as the grains meet some resistance to movement when under stress, grains must change shape so that smooth movement may continue. Since accommodation is a diffusion-controlled process it is enhanced by elevated temperature. It must be kept in mind, however, that higher temperatures also enhance grain growth which, again, counteracts the refinement attained during prior conditioning. Figure 1 graphically depicts the microstructural evolution during TMP.

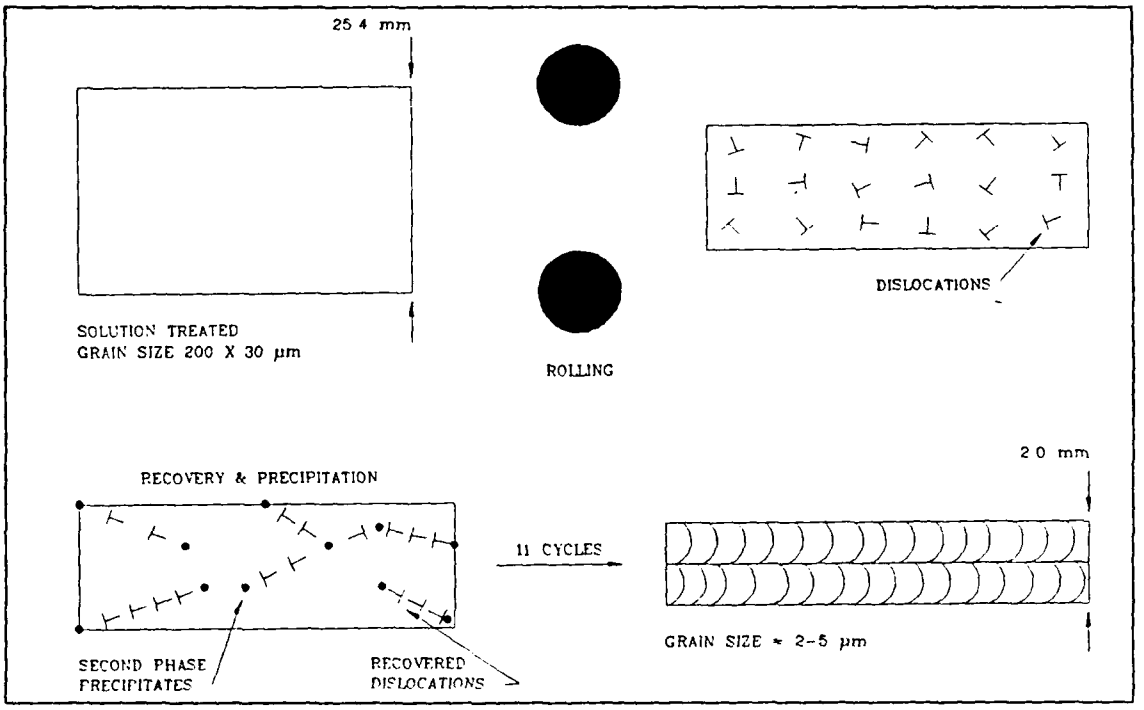

Figure 1. Conditioning via TMP

The effect of altering the TMP variables in an effort to determine the best conditioning procedure will be evaluated by the percent elongation that is achieved during subsequent tensile testing over a range of temperatures and strain rates. The tensile

testing conditions were chosen to represent reasonable superplastic forming (SPF) conditions and to retain highly refined microstructures. This was done by utilizing a high strain rate and lower temperature at which cavitation is minimized.

II. BACKGROUND

A. SUPERPLASTICITY OF AL 7475 TODAY

Superplasticity of Al alloys is of interest primarily because of its potential utilization in aircraft manufacture. By utilizing SPF a manufacturer may make airframe structures and other geometrically complex parts from a single sheet of an Al alloy and thus eliminate the added weight and stress concentration that is inherent with mechanical fasteners and the material property variations resulting from welding. These prospective benefits for aerospace use are the reason this research is supported by Naval Air Systems Command, Washington, DC.

Research on superplasticity in the U.S. has been extensive since the early 1960's and elongations of >1000% have been achieved with some Al alloys. Specifically, previous work done at NPS on Al 7475 by Lee and McNelley achieved 280% elongation at 300°C and a strain rate of 1.7×10^{-3} s^{-1} [Ref. 2: p.255]. Recently, work done by Kobayashi [Ref. 3: p.277] has resulted in elongations in wrought Al 7475 in excess of 800%. Kobayashi's processing was done using the "Rockwell" technique [Ref. 4: p.38] which employs several deformations followed by a single reheating cycle. This 800% elongation occurred at 517°C and a strain rate of 5×10^{-4} s^{-1}, but was accompanied by extensive cavitation in the elongated specimen. Cavitation is the generation of microvoids in a material that is being stressed and renders the material less suitable for future use under load. Cavitation can be suppressed by imposing a large external pressure on the stressed material during SPF but this is expensive and cumbersome for high volume production. Temperature sensitivity was also apparent in Kobayashi's work as maximum elongations dropped to 180% when the test temperature was lowered to 425°C.

A second problem with achieving superplasticity at temperatures in excess of 500°C is the inherent die wear that would exist by SPF at this elevated temperature. This wear problem can only be overcome by utilizing the highest strength steel alloys as die material or lowering the SPF temperature.

B. PHASES PRESENT IN 7475

Al 7475 is a quaternary alloy that yields the highest strengths among the commercial Al alloys [Ref. 5: p.51]. Al 7475 is solution treated at 510°C and has solvus temperatures of ≈420°C for the $Mg(Al,Cu,Zn)_2$ precipitate phase and ≈470°C for the $Mg_3(Al,Cu,Zn)_3$ precipitate phase [Ref. 6]. It is anticipated that one or both of these second phases will precipitate on triple junctions of the dislocation structure during recovery and thus facilitate development of a refined microstructure (≈2-5μm) during conditioning and subsequent SPF.

The use of the precipitates in this manner can be contrasted to their use in tempering to harden prior to service use. During processing relatively large precipitate particles (≈0.5-1μm) are formed at high energy regions of the grain boundaries and at triple points of the substructure. These large precipitates serve to pin the dislocation substructure so that it may stabilize and transform into a refined grain structure.

In contrast to their use in stabilizing the grain structure during processing these same second phases form during tempering of the SPF material for service use. In this instance the SPF material is solution treated again and then given a T6 temper by heating to 120°C for 24 hours [Ref. 7: p.683]. This tempering results in precipitation of the second phase in a dispersion of fine (≈20-35Å), coherent particles that will again interact with dislocations, this time to cause bowing [Ref. 5: p.145]. Then, this precipitate dispersion enhances the materials' strength.

C. GOAL OF THIS PROJECT

The objective of this project is to develop a conditioning procedure utilizing deformation and annealing cycles during TMP that will lead to a refined structure and sufficiently misoriented boundaries to sustain superplastic deformation in the temperature range of 300-400°C. The strain rates utilized in testing ($6.7x10^{-3}$ and $6.7x10^{-4}$ s^{-1}) were chosen to represent strain rates representative of commercial SPF processes.

To this end, several variations of the TMP variables were explored in an effort to identify the most important variables as well as attempt to identify the best conditioning process. The recent work of Kobayashi is used as a measure of success in comparing the results of this project. Optical microscopy will be used to assess the microstructure of the material as well as verify the solution treated grain structure (e.g., grain structure before processing).

III. EXPERIMENTAL PROCEDURE

A. MATERIAL

The material used in this research was aluminum alloy AA number 7475 and was supplied by the Aluminum Company of America (ALCOA), Alcoa Center, Pennsylvania, in 1984. The received material was an 11 in. by 7in. by 1in. (275mm x 175mm x 25mm) wrought plate. This material was chemically analyzed by Anamet Laboratories, Inc., Hayward, California [Ref. 8]. Results of this analysis are shown in Table 1. This composition is within the wt. pct. limits specified for Al 7475.

Table 1. ALLOY COMPOSITION (WT. PCT.)

Al	Zn	Mg	Cu	Cr	Fe	Zr	Si
balance	5.67%	2.29%	1.67%	.20%	.06%	.02%	<.02%

B. PROCESSING

From the received material eight 2.5 in. by 1.0 in. by 1.0 in. (63.5mm x 25.4mm x 25.4mm) experimental billets were sectioned. These billets were initially solution treated by soaking in an air furnace at 473°C for 100 minutes and subsequently solution heat treated at 510°C for 100 minutes followed by a water quench. A section of the solution treated alloy was examined under the optical microscope to ensure that the precipitated phases had completely dissolved into solution and that no grain boundary melting had taken place.

At this point the 8 billets underwent different TMPs (lettered A-H) and various possible comparisons between TMP's are summarized in Table 2. The asterisks indicate the TMP variable being compared in each section of the table. The overaged billets were held at 300°C for 12 hours and then water quenched *prior to any rolling*. The reduced

rolling temperature was applied only on the last 5 passes through the rolling mill. This was accomplished by taking the billet out of the reheating furnace and placing it in a furnace at a lower temperature for 5 minutes of equilibration preceding the rolling.

Table 2. PROCESSING SCHEDULE COMPARISONS

TMP	Overaged @ 300°C for 12 hours (Yes or No)	Time between rolling passes (min.)	Temperature of last 5 passes (°C)	Reheating temperature (°C)	True strain (ε)
A	No	30*	300	300	2.47
B	No	4*	300	300	2.46
A	No	30	300*	300	2.47
D	No	30	250*	300	2.62
E	No	30	20*	300	2.55
H	No	30	150*	300	2.56
F	Yes*	30	150	300	2.58
H	No*	30	150	300	2.56
F	Yes	30	150	300*	2.58
G	Yes	30	150	375*	2.56
C	No	30	250	300	2.71

The rolling was conducted in the same direction as the rolling direction during original fabrication of the plate. Earlier research at NPS by Groh [Ref. 9: p.56] on Al 2090 showed that this facilitated the processing. The rolling was done on a Fenn rolling mill with 6 in. (15.2cm) wide by 4.25 in. (10.8cm) diameter steel rolls rotating at $\approx$ 20 RPM. The final true rolling strain(ε) was between 2.46 (final thickness$\approx$2.18mm) and 2.71 (final thickness$\approx$1.69mm). When one furnace was used during rolling the billets were heated in a Blue M furnace and when two temperatures were utilized during the rolling reheating process the Blue M was used for the higher temperature heating and a Lindberg laboratory box furnace was used for the lower temperature heating. Both

furnaces had steel plates covering the hearth of the furnace to act as heat sinks to maintain temperature during openings of the door. The furnace temperatures were monitored by two Chromel-Alumel thermocouples and maintained within 3°C of the specified temperature. The billets were preheated for 30 minutes prior to the first rolling pass and the reduction schedule was similar for all of the experimental billets and as specified in Table 3.

Table 3. REDUCTION SCHEDULE

Pass number	Pre-pass thickness (mm)	Reduction (mm)	% of original thickness	% of previous thickness	Post-pass thickness (mm)
1	25.40	3.00±.05	11.8	11.8	22.40
2	22.40	2.60±.05	10.2	11.6	19.80
3	19.80	2.60±.05	10.2	13.1	17.20
4	17.20	2.60±.05	10.2	15.1	14.60
5	14.60	2.60±.05	10.2	17.8	12.00
6	12.00	2.60±.05	10.2	21.7	9.40
7	9.40	2.60±.05	10.2	27.7	6.8
8	6.80	1.55±.05	6.1	22.8	5.25
9	5.25	1.30±.05	5.1	24.8	3.95
10	3.95	1.15±.05	4.5	29.1	2.80
11	2.80	0.80±.05	3.1	28.6	2.00±.35

C. TESTING

The elongated sheet of processed material was then machined into tensile test samples blanks. These machined blanks were 2.0 in. (50.8mm) long and 0.5 in. (12.7mm) in width. The tensile test samples were machined from these blanks with a gage section of 0.5 in. (12.7mm), gage width of 0.2 in. (5.1mm) and shoulder radius of 0.06 in. (1.5mm).

These machined samples were then tensile tested using an Instron floor-model (TT-D) tensile testing machine with a three zone clamshell furnace maintaining the test temperature. The test temperature was *monitored* by six Chromel-Alumel thermocouples. These thermocouples were mounted vertically 1.0 in. (25.4mm) apart across the 5.0 in. (127mm) extent of the sample and grips to ensure that no temperature gradients were present during the tensile test.

The test samples were placed in pre-heated holding grips and then placed between the Instron crosshead mounts. The pre-heated clamshell furnace was then closed around the test sample assembly. The test sample reached equilibrium at the test temperature in approximately 25 minutes after insertion and the tensile tests were then started. The tensile testing was conducted at temperatures of 300 to 450°C and strain rates of $6.7x10^{-3}$, $6.7x10^{-4}$ and $6.7x10^{-5}$ s^{-1}. The resultant load versus time plots provided by the Instron machine were used to obtain data points that were used to calculate true stress (σ) and true strain (ε). The plots of σ versus ε are collected in Appendix A.

D. MICROSCOPY

Metallurgical examination of the tested material was conducted under the optical microscope at various magnifications up to 715X. Preparation of the material for microscopic examination was as follows. The optical sample was mounted in an acrylic mold and then progressively smoothed on sand paper ranging from 240 to 600 grit. The samples were then polished on nylon covered wheels using 6μm, 3μm and 1μm particle size diamond paste successively. After polishing on each wheel the sample was etched with Keller's reagent [Ref. 10: p.354] for 30 seconds and ultrasonically cleaned in ethanol for 60 seconds. Final polishing was done with a slurry of cerium oxide and water on a Microcloth wheel. Lastly, the sample was etched with Keller's reagent for $\approx$10-15 seconds prior to microscopic viewing.

IV. RESULTS

A. MECHANICAL PROPERTIES OF THE PROCESSED MATERIAL

The original experimental plan called for tensile testing between 300 and 450°C in 50°C increments and at strain rates of 6.7×10^{-3} or 6.7×10^{-4} s^{-1}. After TMP's A and B tensile test data were evaluated, the 450°C testing was abandoned on subsequent TMP's because the data indicated that the greatest elongations were obtained at 350°C and thus a 450°C test was unnecessary. The complete data for elongations at various testing conditions is compiled in Table 4. When multiple tests were conducted at certain conditions only the highest elongation result is reported in the table.

Noteworthy additions to the testing program are 3 additional tensile tests conducted as follows: TMP D at temperature of 350°C and strain rate of 6.7×10^{-5} s^{-1}; TMP F at 300°C and strain rate of 6.7×10^{-5} s^{-1}; and TMP G at 450°C and strain rate of 6.7×10^{-3} s^{-1}. These additional tests were suggested by the data trends observed.

The load versus time plots provided by the Instron tensile testing machine were reduced to true stress (σ) versus true strain (ε) plots and these are gathered in Appendix A. The σ versus ε plots were then utilized to determine a value of σ at $\varepsilon = 0.1$ and a plot of the log σ at $\varepsilon = 0.1$ versus log ε was developed for each testing condition and these data are gathered in Appendix B.

Table 4. ELONGATIONS AT TENSILE TEST TEMPERATURES

TMP Batch/ Strain Rate (1/SEC)	300°C	350°C	400°C	450°C
TMP A/ 6.7x10-3	90%	133%	145%	143%
TMP A/ 6.7x10-4	109%	169%	116%	107%
TMP B 6.7x10-3	117%	166%	145%	127%
TMP B 6.7x10-4	125%	173%	91%	83%
TMP C 6.7x10-3	117%	177%	163%	---
TMP C 6.7x10-4	139%	219%	81%	---
TMP D 6.7x10-3	95%	165%	135%	---
TMP D 6.7x10-4	118%	285%	109%	---
TMP D 6.7x10-5	---	206%	---	---
TMP E 6.7x10-3	89%	163%	143%	---
TMP E 6.7x10-4	161%	180%	97%	---
TMP F 6.7x10-3	179%	193%	139%	---
TMP F 6.7x10-4	195 %	167%	105%	---
TMP F 6.7x10-5	199%	---	---	---
TMP G 6.7x10-3	101%	179%	239%	199%
TMP G 6.7x10-4	131%	191%	107%	---
TMP H 6.7x10-3	125%	221%	143%	---
TMP H 6.7x10-4	185%	193%	99%	---

B. INFLUENCE OF PROCESSING ON MICROSTRUCTURE

The solution treated material had elongated grains approximately 200 by 30μm in size. This microstructure is shown in Figure 2 and is similar to wrought 7xxx series solution treated alloys pictured in, for example, the Metals Handbook [Ref. 10: p.369]. No eutectic melting occurred and this is also evident in the appearance of the solution treated material in Figure 2.

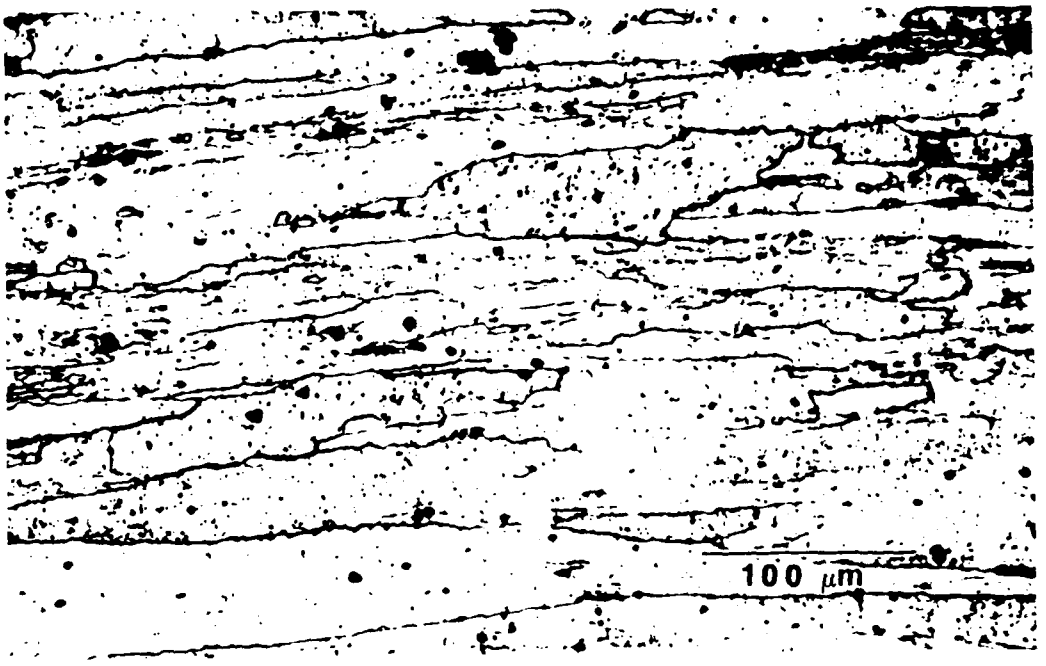

Figure 2. Micrograph of Solution Treated material (285X)

The processed material was expected to exhibit a refined microstructure with a dispersion of precipitated intermediate particles. The refined microstructure is apparent in Figure 3. The size of this refined structure is not discernible at this magnification but is assumed to be $\approx$2-5μm as was obtained in similar processing of Al 2090 by Groh [Ref. 9: p.40]. The precipitate dispersion is best seen in a micrograph of greater magnification shown in Figure 4. This figure shows fine precipitation that is assumed to be both the

$Mg(Al,Cu,Zn)_2$ and $Mg_3(Al,Cu,Zn)_5$ phases. It is also evident in Figure 4 that two differently sized precipitates evolved during processing. TEM examination is needed to determine the compositions as well as if they are the two different phases or just size differences of one precipitate phase.

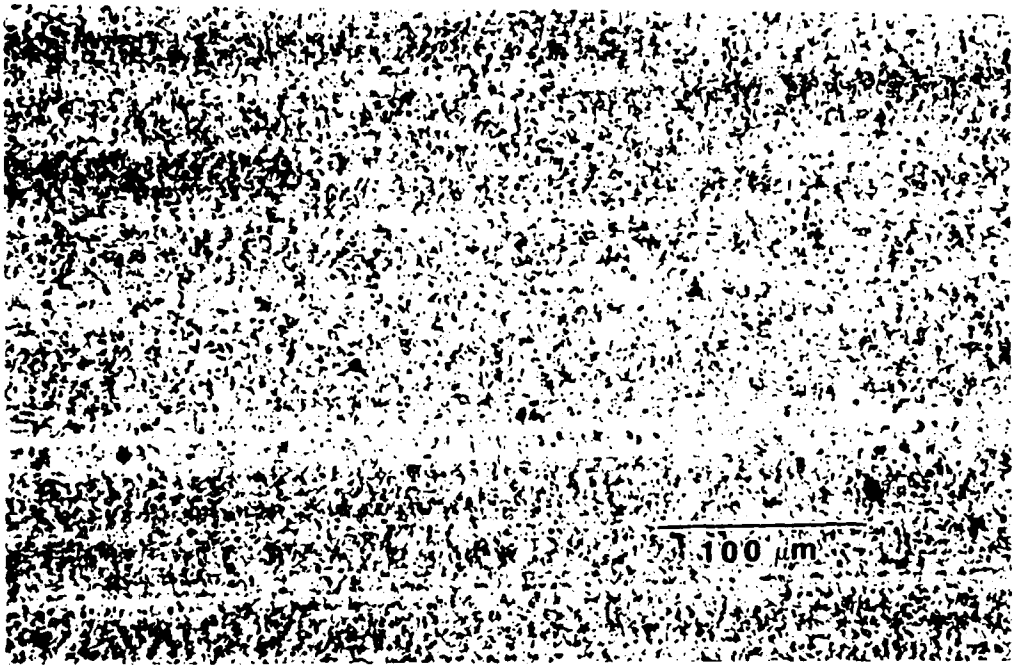

Figure 3. Micrograph of Processed material (285X)

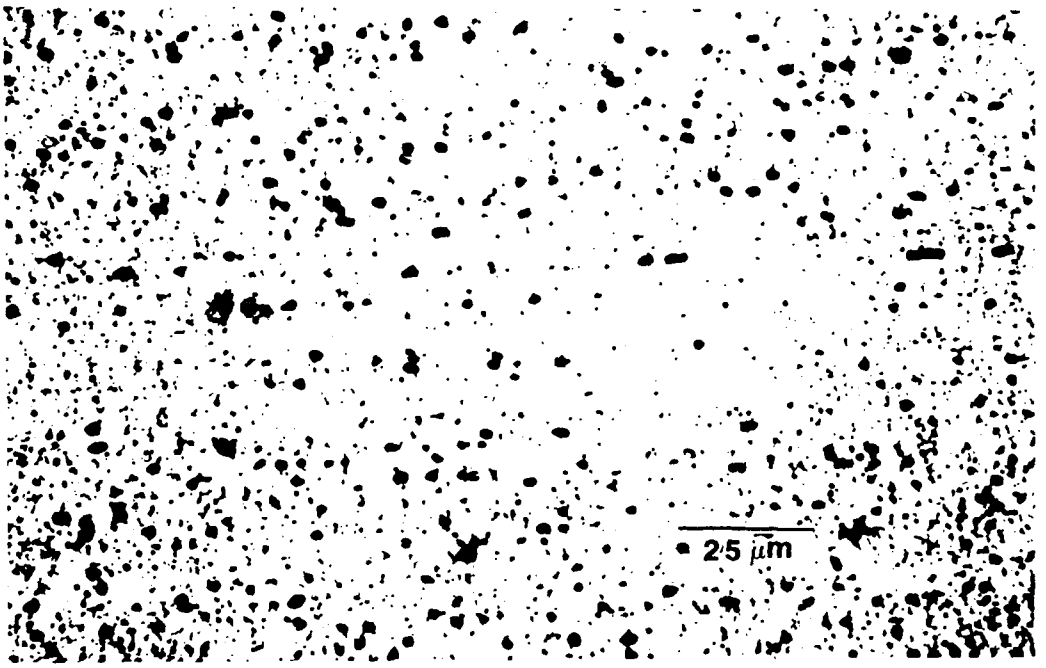

Figure 4. Micrograph of Processed material (715X)

The tensile test sample that had the greatest elongation (285%) displayed a refined microstructure similar in appearance to the post processing microstructure with the following differences. Missing from the deformed material, Figure 5, is the longitudinal directionality that is seen in Figure 3. Figure 5, which was taken in the gage section of the tensile test sample near fracture, also shows signs of cavitation that were not present in the material before deformation. At greater magnification (Figure 6) the refined microstructure, precipitate dispersion, and cavitation are again seen.

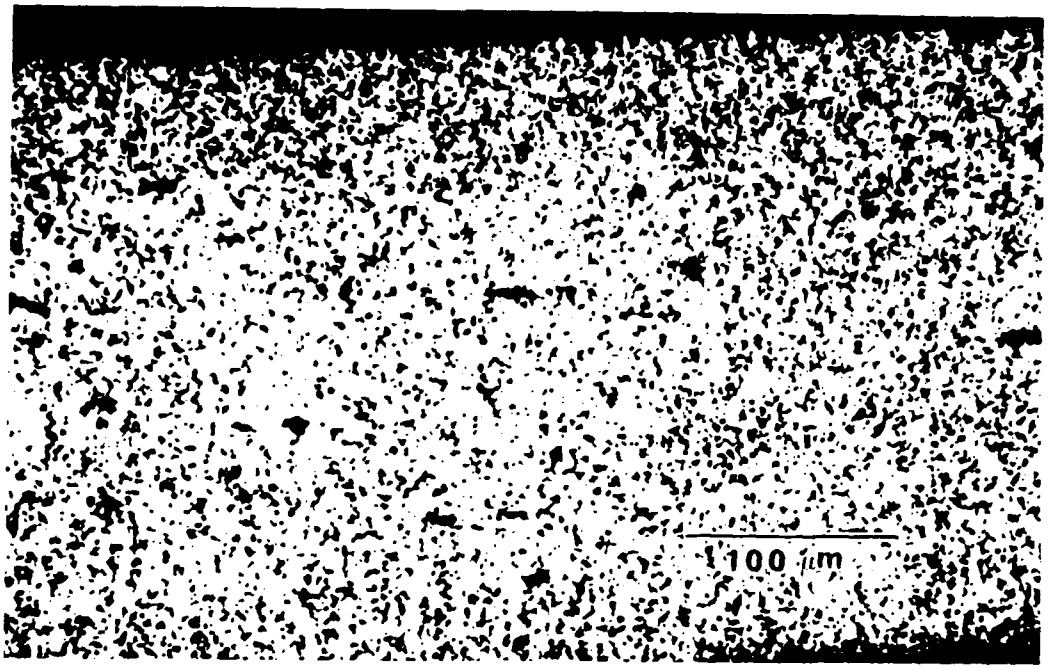

Figure 5. Micrograph of Processed and Elongated material (285X)

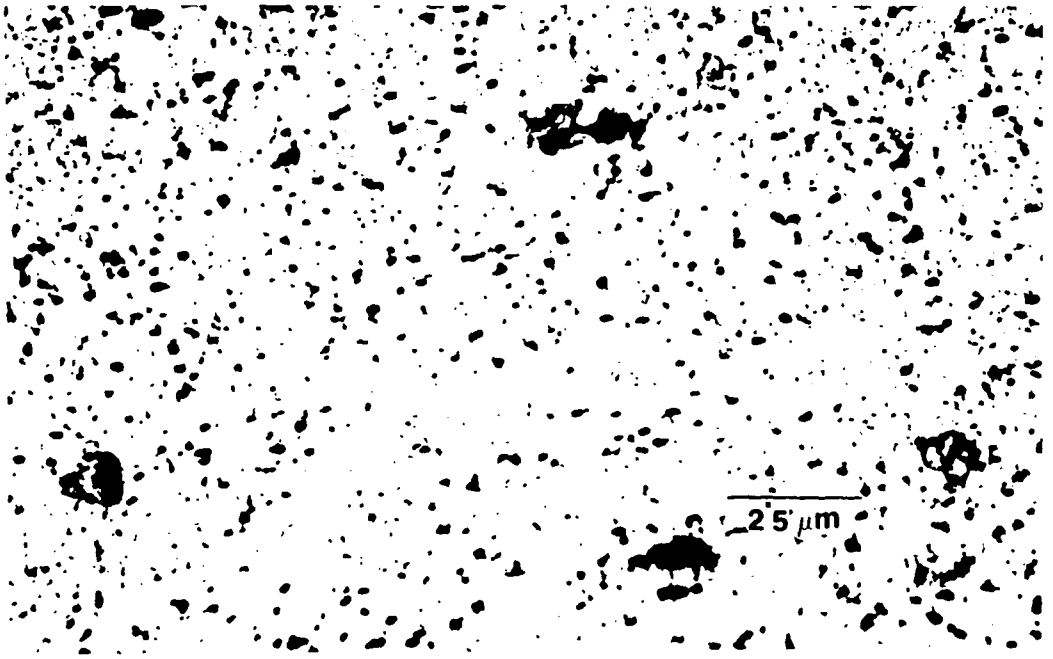

Figure 6. Micrograph of Processed and Elongated material (715X)

C. DISCUSSION AND CONCLUSIONS

Review of Table 4 indicates that few processing conditions resulted in superplastic ductility. The maximum elongation attained was 285%, in material processed by TMP D and tested at 350°C and a strain rate of 6.7×10^{-4} s^{-1}.

The first conclusion drawn from the results of this project is that the reheating interval did not have an effect on percent elongation in subsequent testing. Previous work done on Al alloy 2090 by Groh [Ref. 9: p.23] and work done on the Al-10Mg alloy [Ref. 1: p.66] concluded that greater elongations were achieved with a 30 minute reheating interval between rolling passes when compared to a 4 minute reheating interval between rolling passes. This improvement in superplastic ductility with increased reheating time was attributed to the more fully developed grain boundary structure of sufficient misorientation to sustain the superplastic deformation mechanism. That is, the increased heating interval allowed more recovery to take place and subsequently greater stabilization of the refined microstructure. The same result was anticipated with Al 7475 but Figure 7 indicates that this was not the case. This conclusion reinforces the tenet that although Al alloys are often grouped together there can be great differences in their behavior depending on the constituency of the alloying elements, both in type and amount.

A second conclusion is that reduced rolling temperatures (<300°C) have a beneficial effect on percent elongation. We postulate that greater elongations are achieved when lower rolling temperatures are utilized. This increased elongation is attributed to the increased dislocation density caused by putting more work into the material (e.g., by rolling at a lower temperature). This increased dislocation density provides more dislocations for development of the refined grain structure and contributes to evolution of the

refined microstructure by increasing the grain boundary misorientation. This effect enhances superplastic deformation. The same result was expected with Al 7475 and Figure 8 graphically shows that this was indeed the case.

A third conclusion is that the 350°C tensile testing temperature was best suited for achieving superplasticity in Al 7475. This is borne out by observing the elongations in Table 4 and the scatterplot of this projects results in Figure 9. A similar result was reported by Groh in work with Al 2090 [Ref. 9: p.23]. The likely reason for this is that a certain temperature strikes a balance in the diffusion rate with increased microstructural coarsening. That is, at an optimum temperature, in this case 350°C, enough diffusion occurs so that accommodation transpires smoothly between the sliding grains while concurrent grain growth is minimized. At temperatures greater than 350°C excessive growth interrupts the sliding phenomenon (e.g., superplasticity) by increasing accommodation diffusion distances while temperatures less than 350°C inhibit the diffusion necessary for the accommodation process. Both of these cases result in lower percent elongations and are therefore not optimal.

Lastly, it is useful to compare the results obtained here with those of other researchers. It was found that significantly higher elongations at the test temperature of 350°C (maximum elongation = 285%) were possible when the material was subjected to lower rolling temperatures during TMP. This is illustrated graphically in Figure 9 which shows the percent elongations reported by Kobayashi [Ref. 3: p.277] in 1988 to be falling below 185% at the test temperature of 425°C while this project elicited higher elongation in the range of 300 to 400°C, especially at 350°C. This rise in elongation is attributed to a relative grain refinement achieved by TMP done in this project compared to Kobayashi. These fine grains may be able to slide and accommodate more readily than the relatively large grains (12-15μm) that were products of Kobayashi's processing.

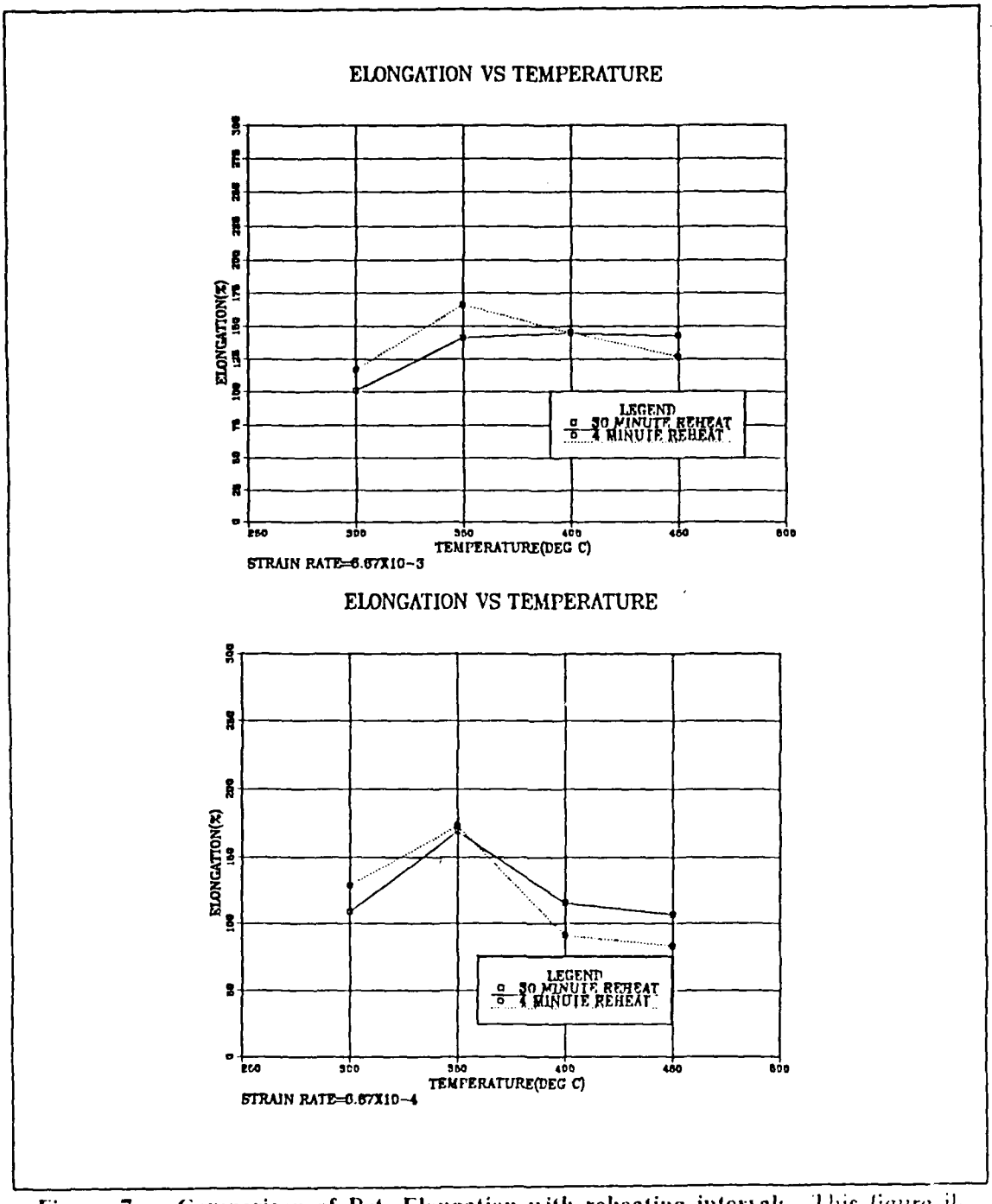

Figure 7. Comparison of Pct. Elongation with reheating interval: This figure illustrates that no discernible difference was found between the reheating intervals of 30 minutes and 4 minutes.

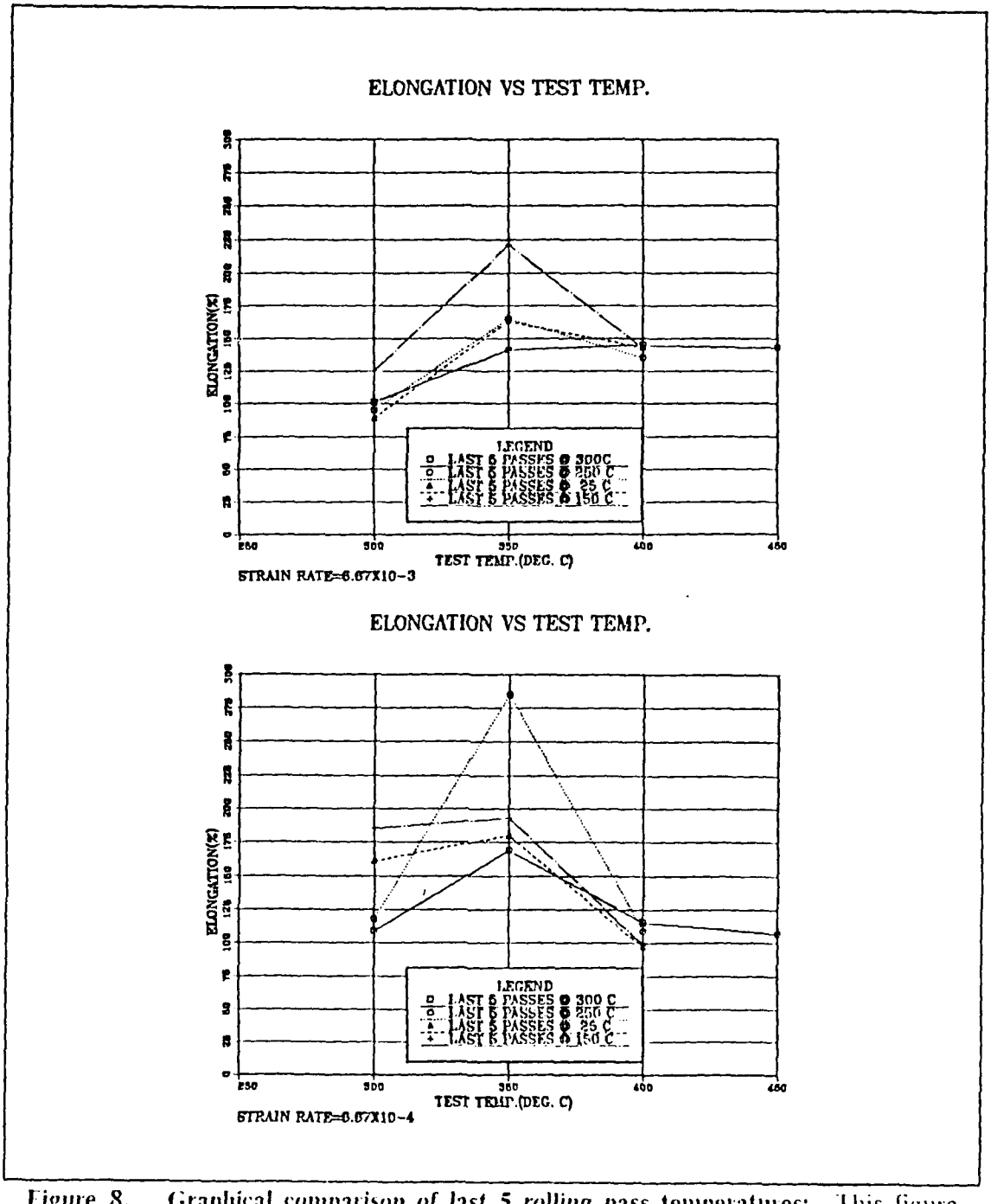

Figure 8. ***Graphical comparison of last 5 rolling pass temperatures:*** This figure shows that lowering the rolling temperature on the last 5 passes had a beneficial effect on pct. elongation during tensile testing. Note that the best elongations were obtained at different last pass rolling temperatures for each strain rate.

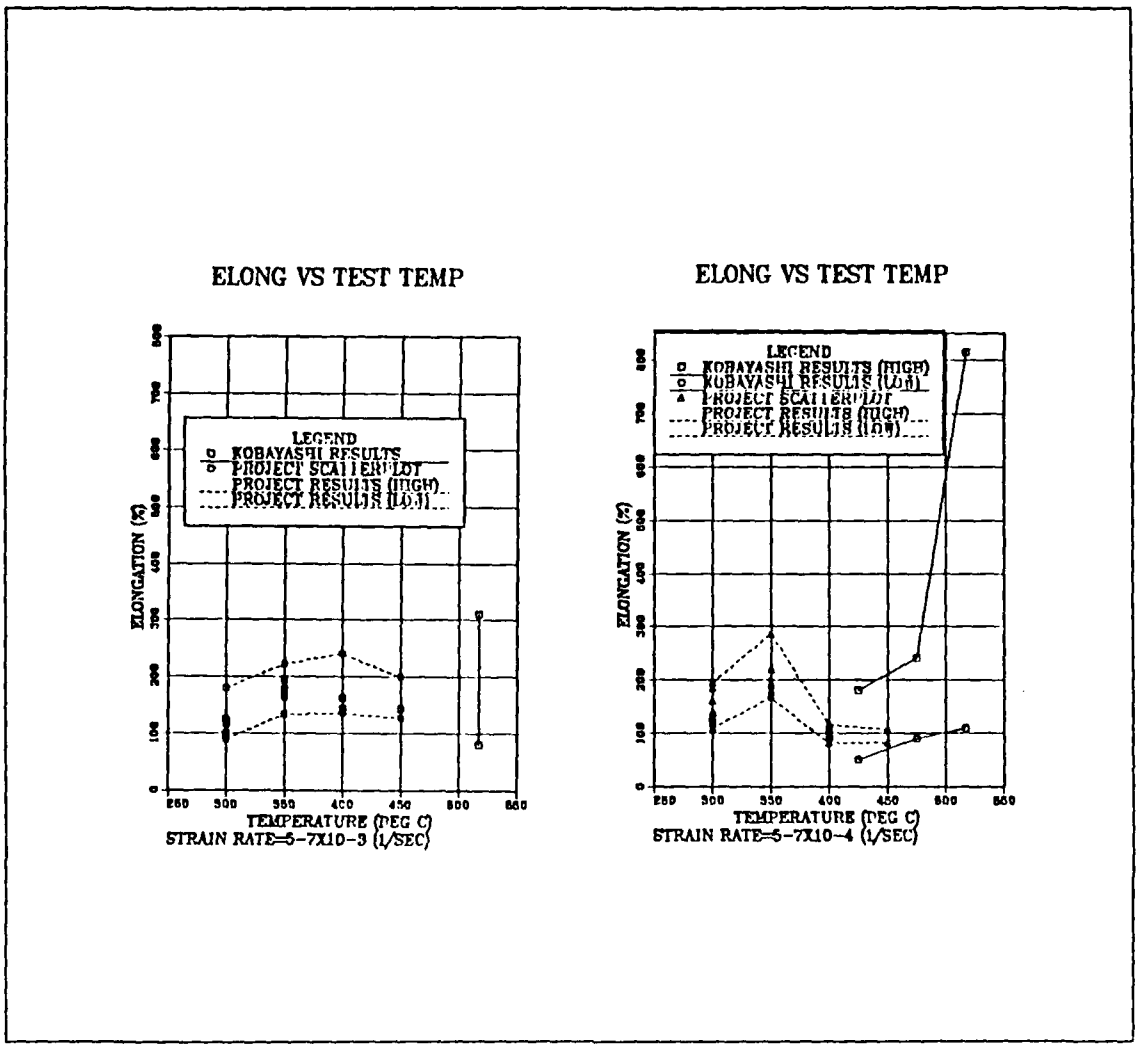

Figure 9. Illustration of Results Comparison: This figure illustrates the results of this project as compared with those obtained by Kobayashi. The results of this project are comparable with those of Kobayashi's work at strain rate of $5\text{-}7\text{x}10^{-3}\ s^{-1}$ and indicate that this project elicited greater elongation at lower temperatures than the trend of Kobayashi's results for the $5\text{-}7\text{x}10^{-4}\ s^{-1}$ strain rate.

V. RECOMMENDATIONS

1. Further analysis with the TEM to determine substructure, grain size, and especially boundary misorientation achieved through processing.

2. Further analysis with the TEM of the phase(s) precipitated during processing. This should allow a determination of whether one phase is more prevalent than the other and whether one phase is more active in stabilizing the refined grain structure than the other.

3. Further investigation into the effects of overaging and higher reheating temperatures on percent elongation. This investigation should involve the use of TEM observations.

APPENDIX A. PLOTS OF TRUE STRESS VS TRUE STRAIN

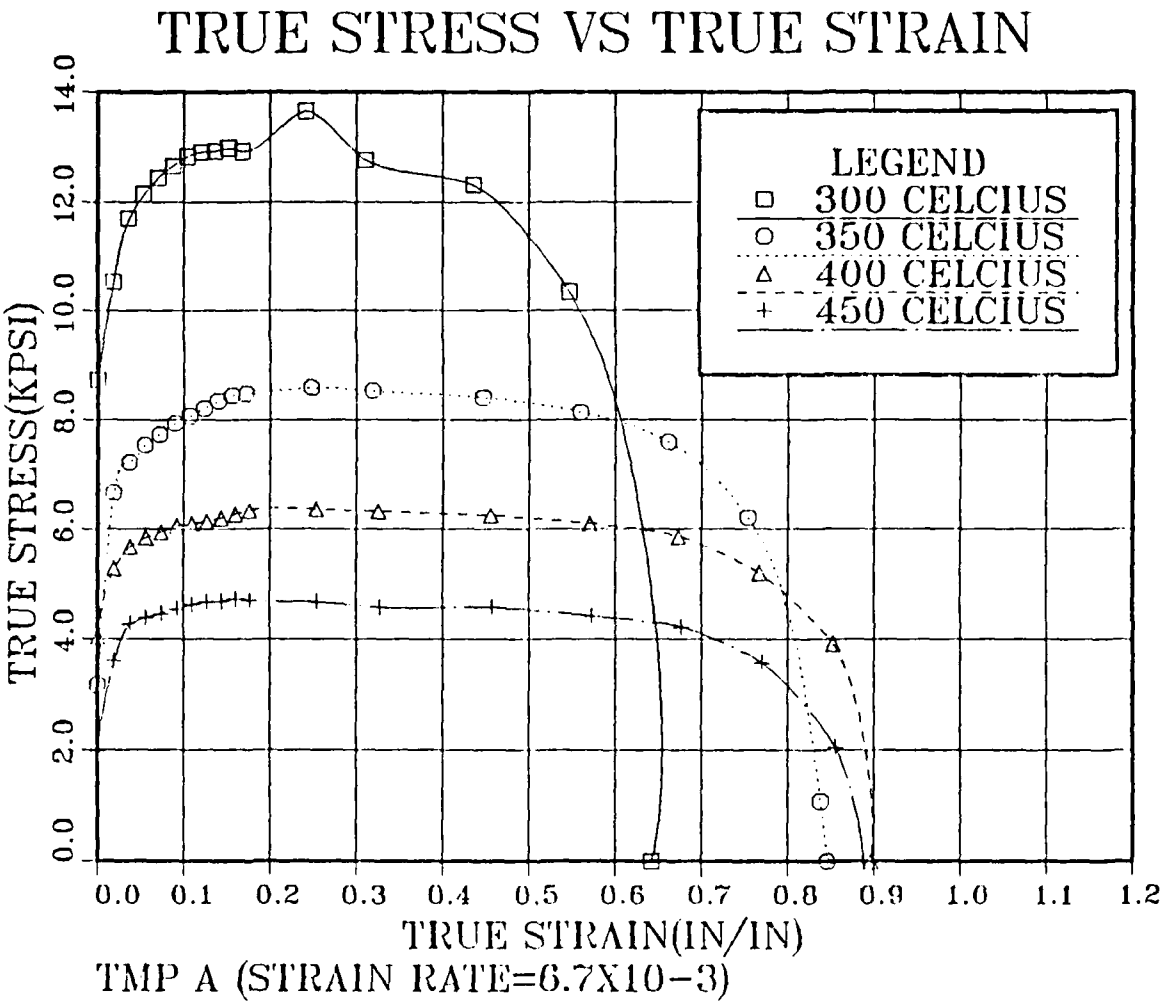

Figure 10. **True Stress vs True Strain for material processed by TMP A:** These data were obtained as a function of test temperature for strain rate of $6.7 \times 10^{-3}\ s^{-1}$.

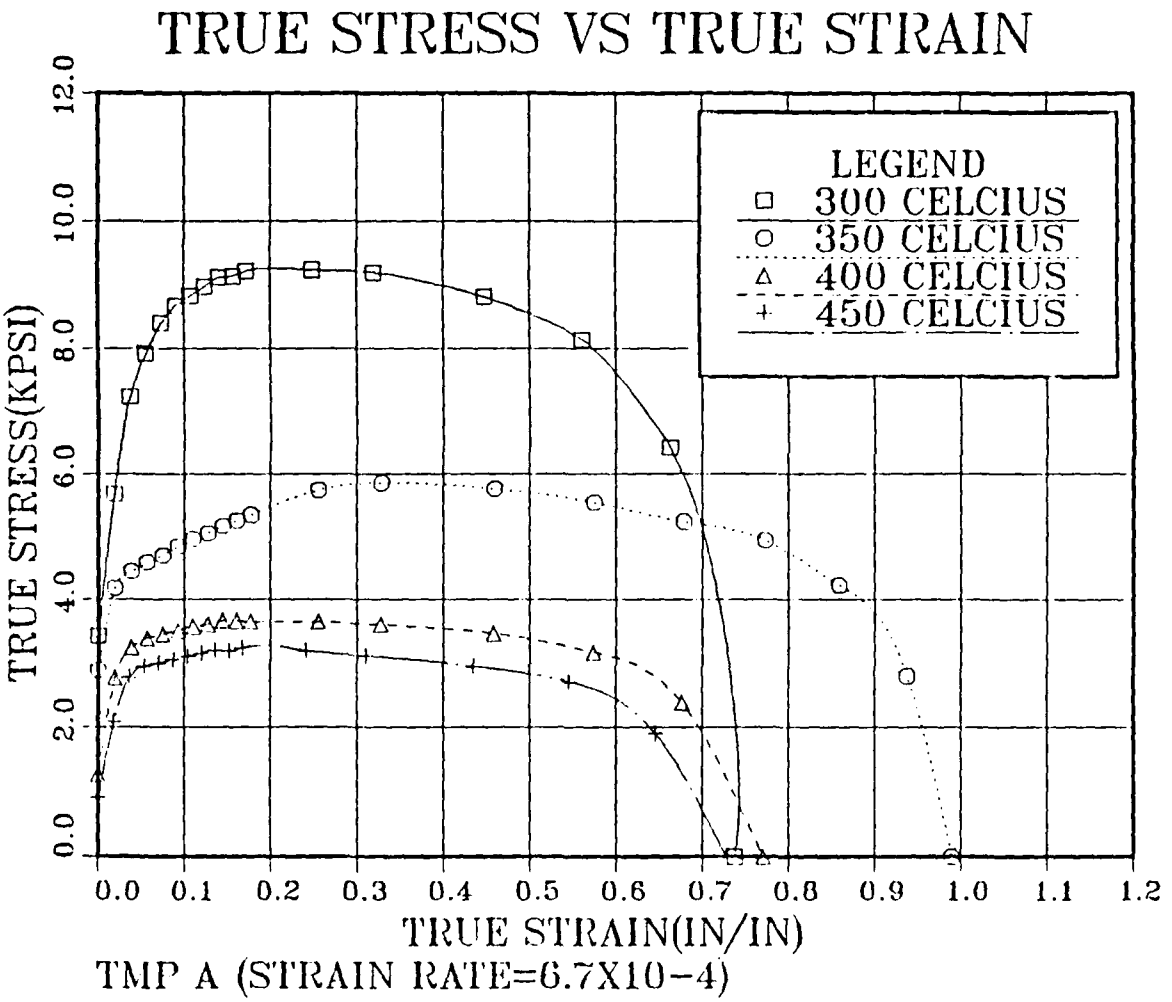

Figure 11. True Stress vs True Strain for material processed by TMP A: These data were obtained as a function of test temperature for strain rate of 6.7×10^{-4} s^{-1}.

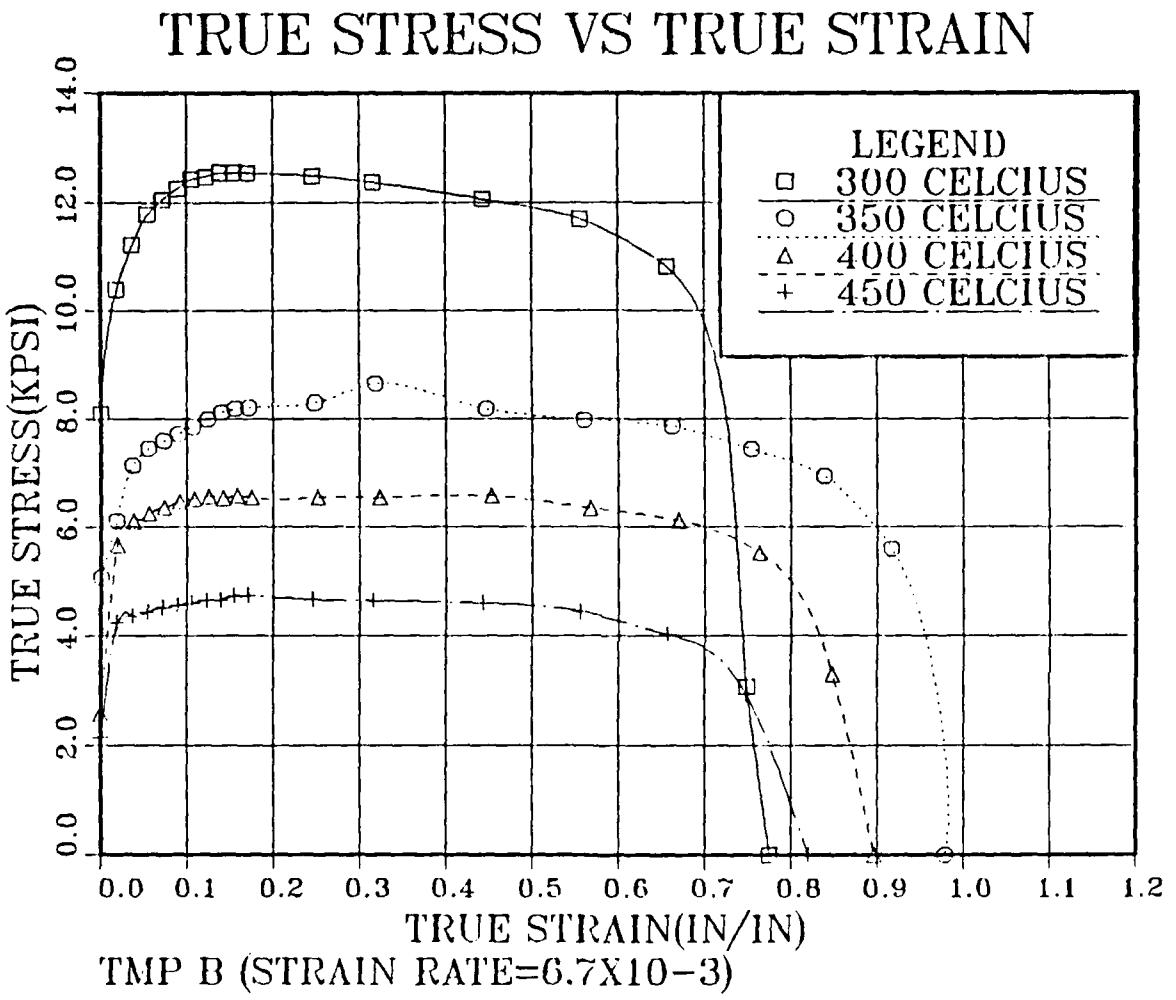

Figure 12. True Stress vs True Strain for material processed by TMP B: These data were obtained as a function of test temperature for strain rate of $6.7 \times 10^{-3}\ s^{-1}$.

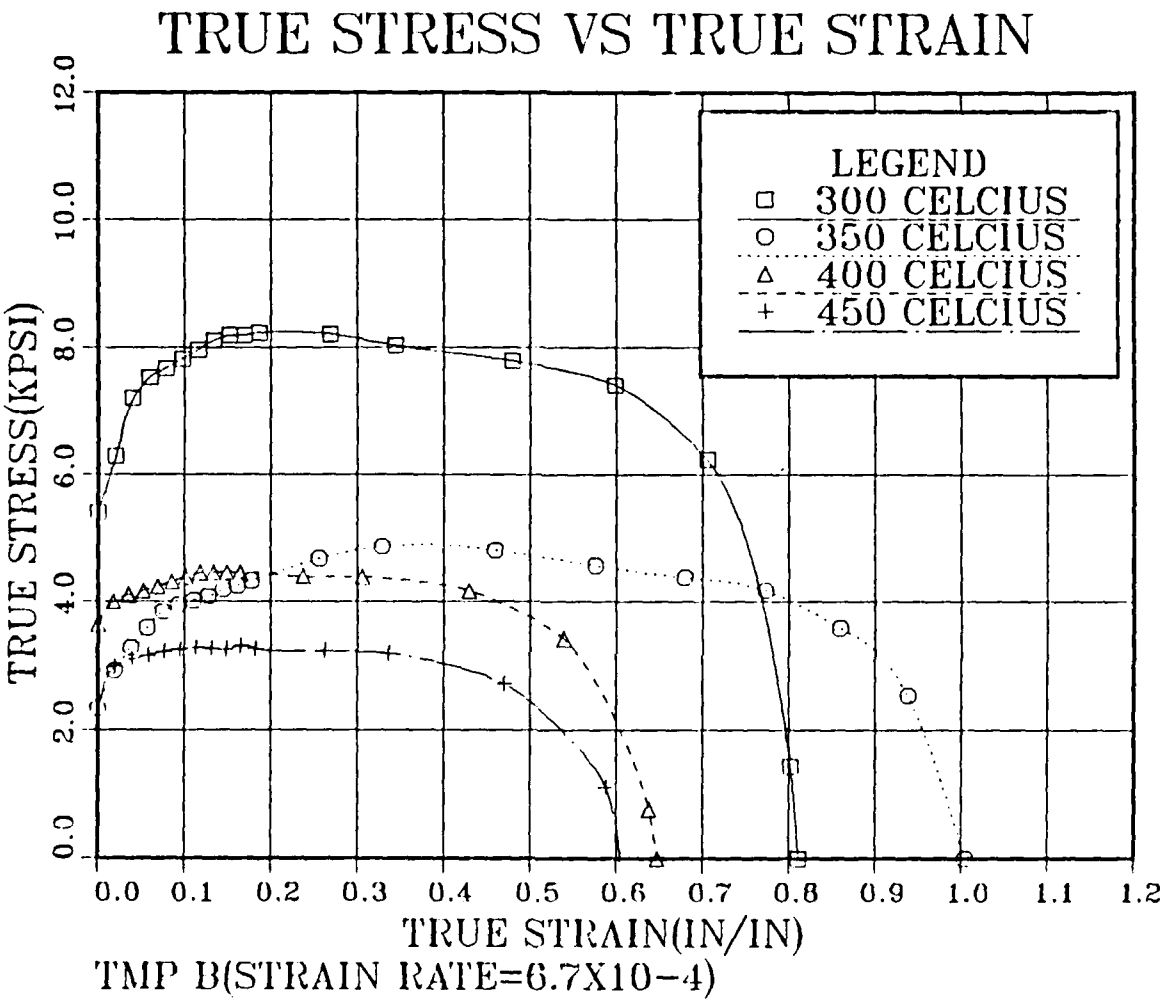

Figure 13. True Stress vs True Strain for material processed by TMP B: These data were obtained as a function of test temperature for strain rate of $6.7 \times 10^{-4}\ s^{-1}$.

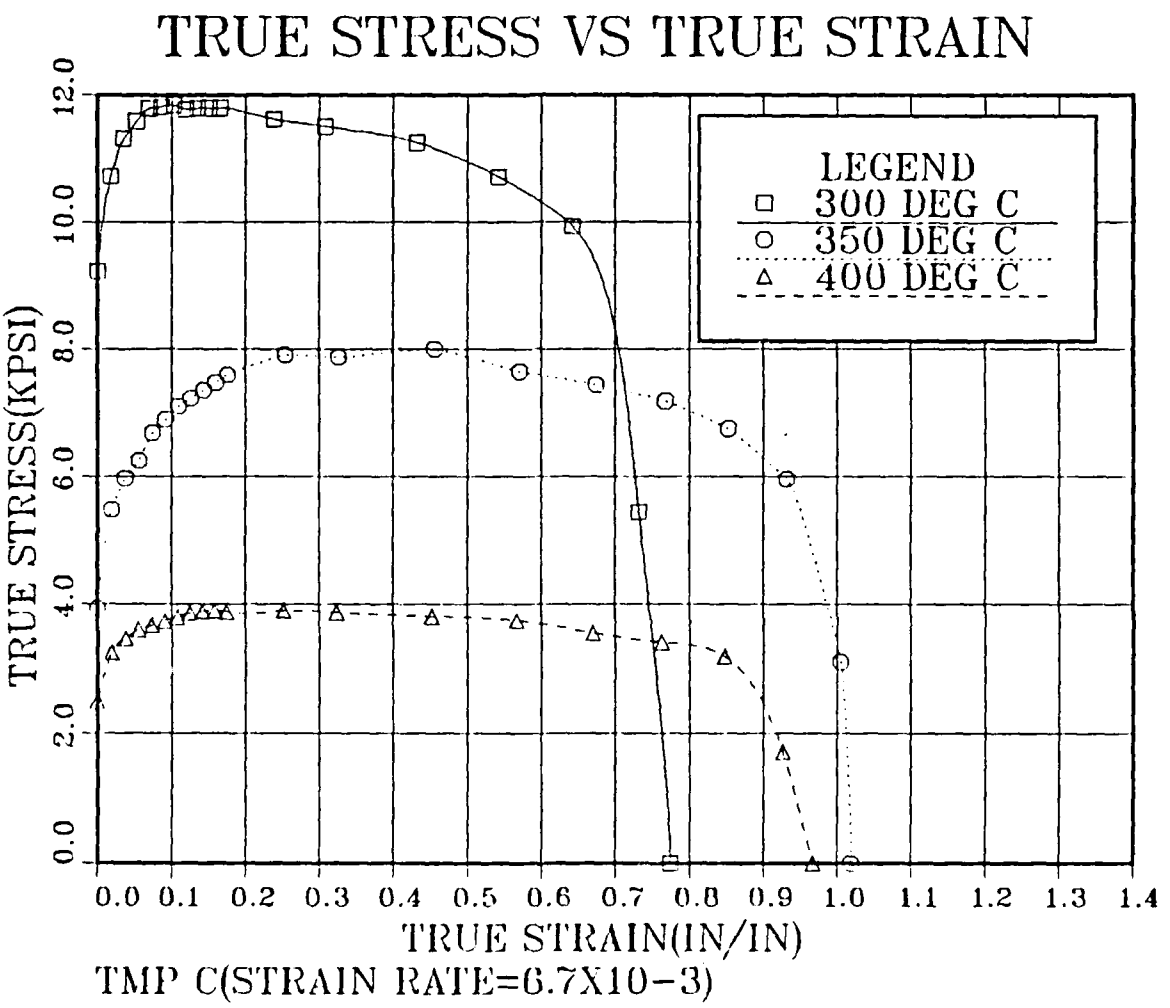

Figure 14. True Stress vs True Strain for material processed by TMP C: These data were obtained as a function of test temperature for strain rate of $6.7 \times 10^{-3}\ s^{-1}$.

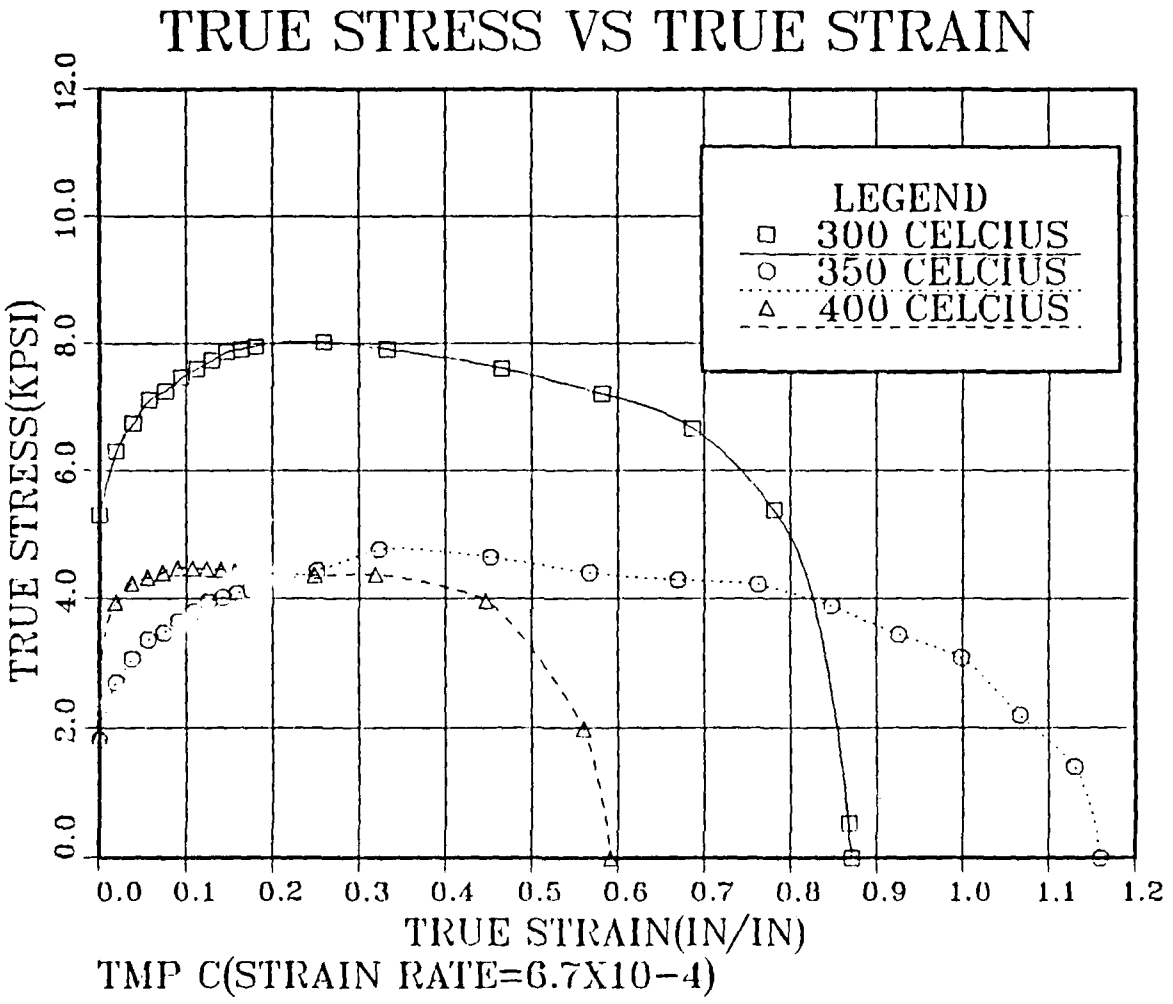

Figure 15. True Stress vs True Strain for material processed by TMP C: These data were obtained as a function of test temperature for strain rate of 6.7×10^{-4} s^{-1}.

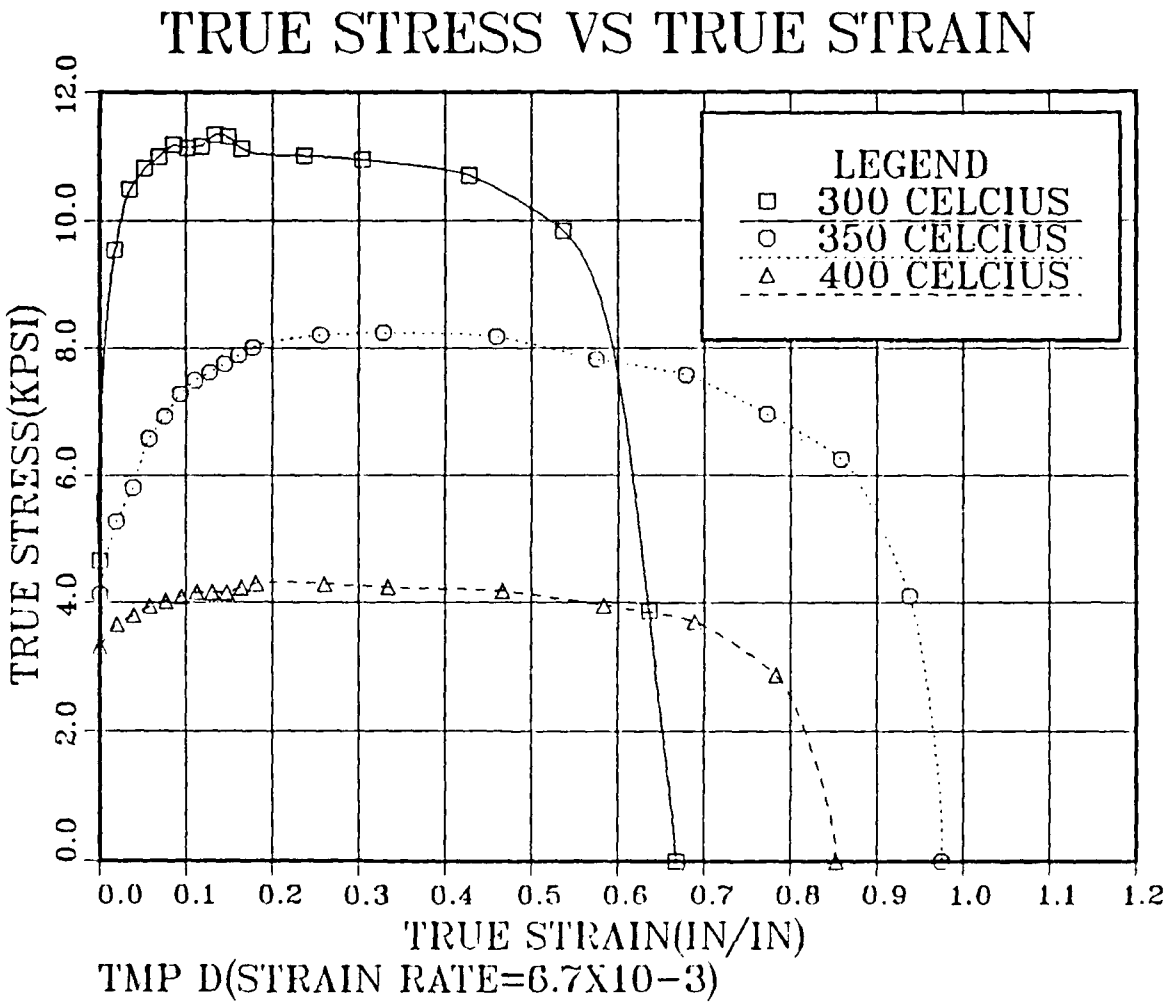

Figure 16. True Stress vs True Strain for material processed by TMP D: These data were obtained as a function of test temperature for strain rate of $6.7 \times 10^{-3}\ s^{-1}$.

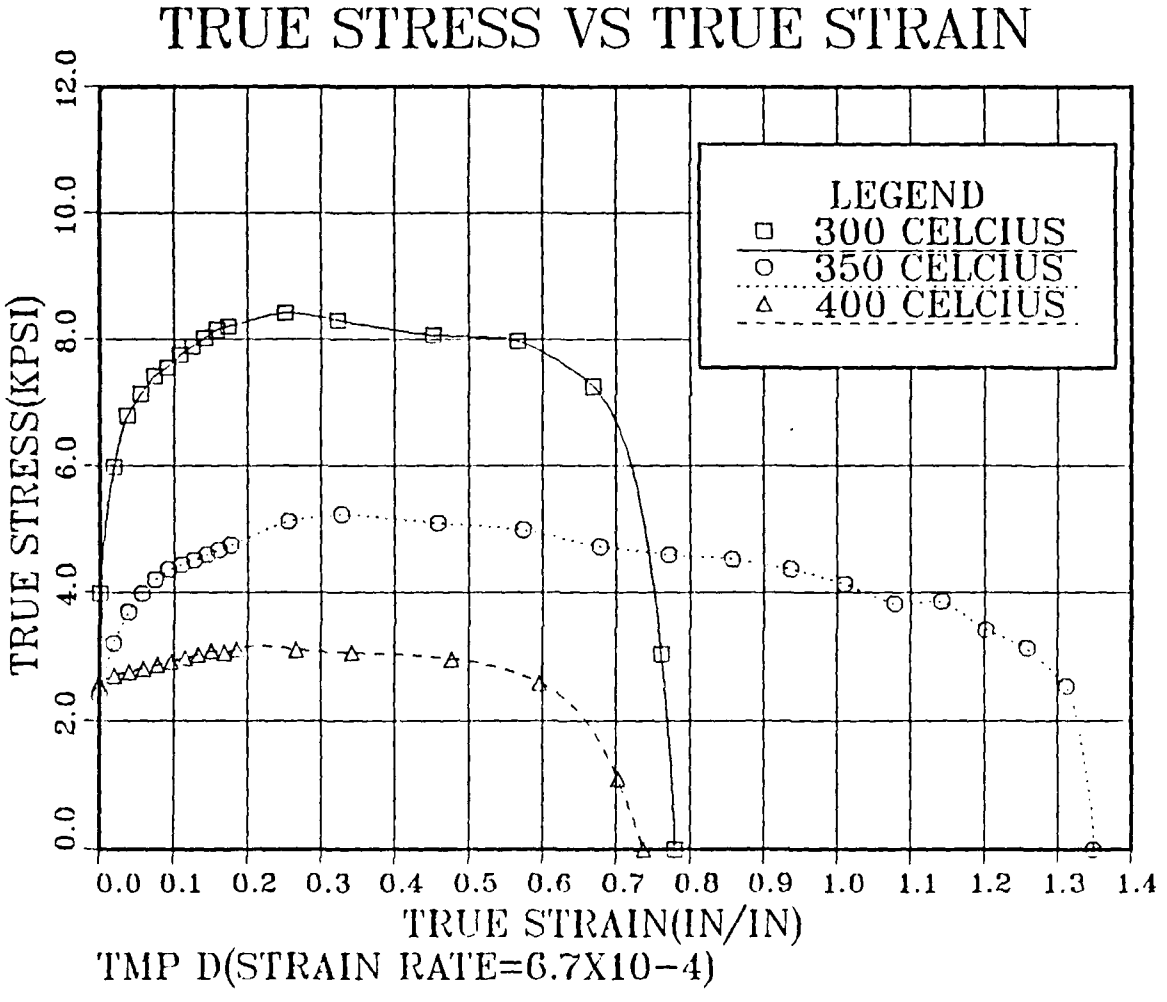

Figure 17. True Stress vs True Strain for material processed by TMP D: These data were obtained as a function of test temperature for strain rate of 6.7×10^{-4} s^{-1}.

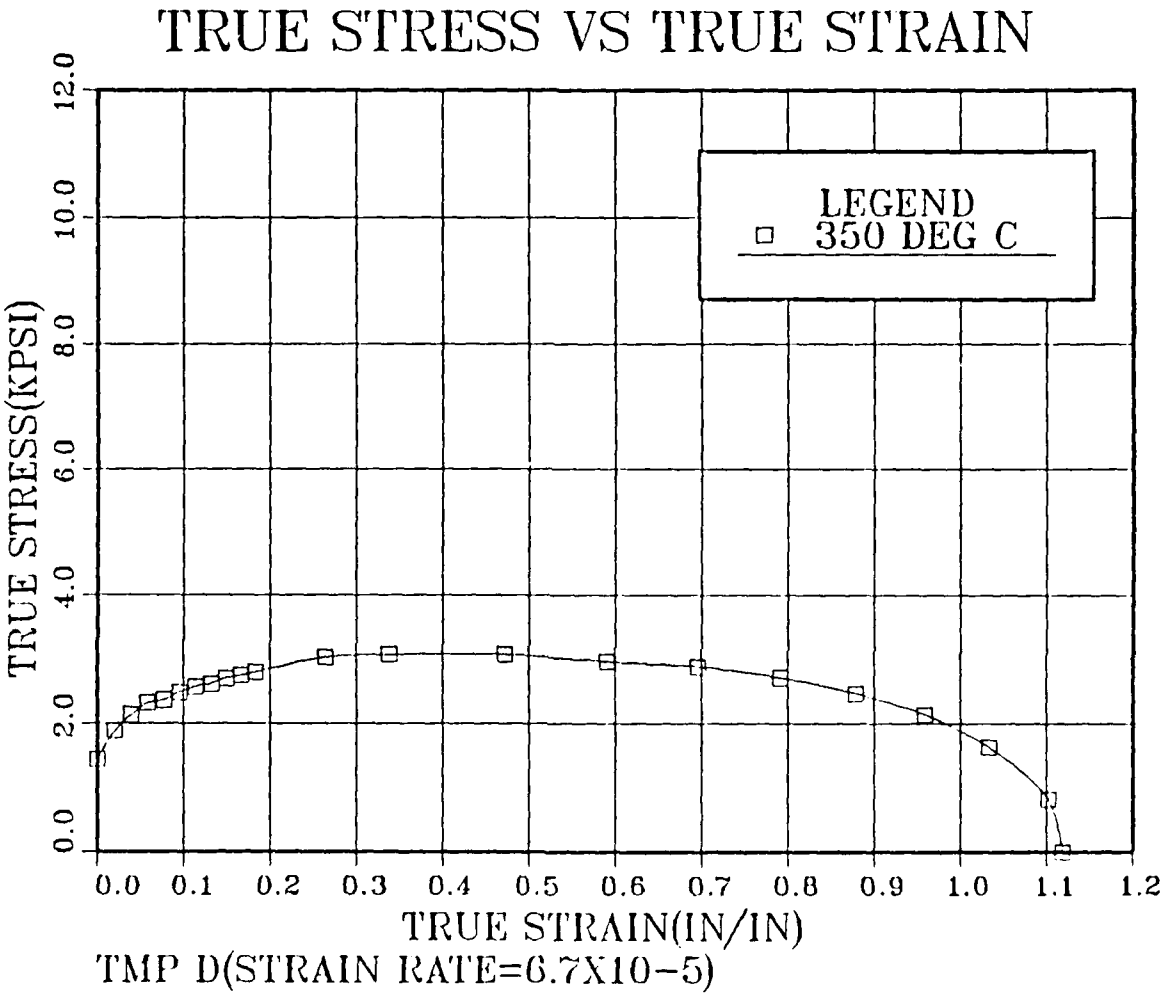

Figure 18. True Stress vs True Strain for material processed by TMP D: These data were obtained as a function of test temperature for strain rate of 6.7×10^{-5} s^{-1}.

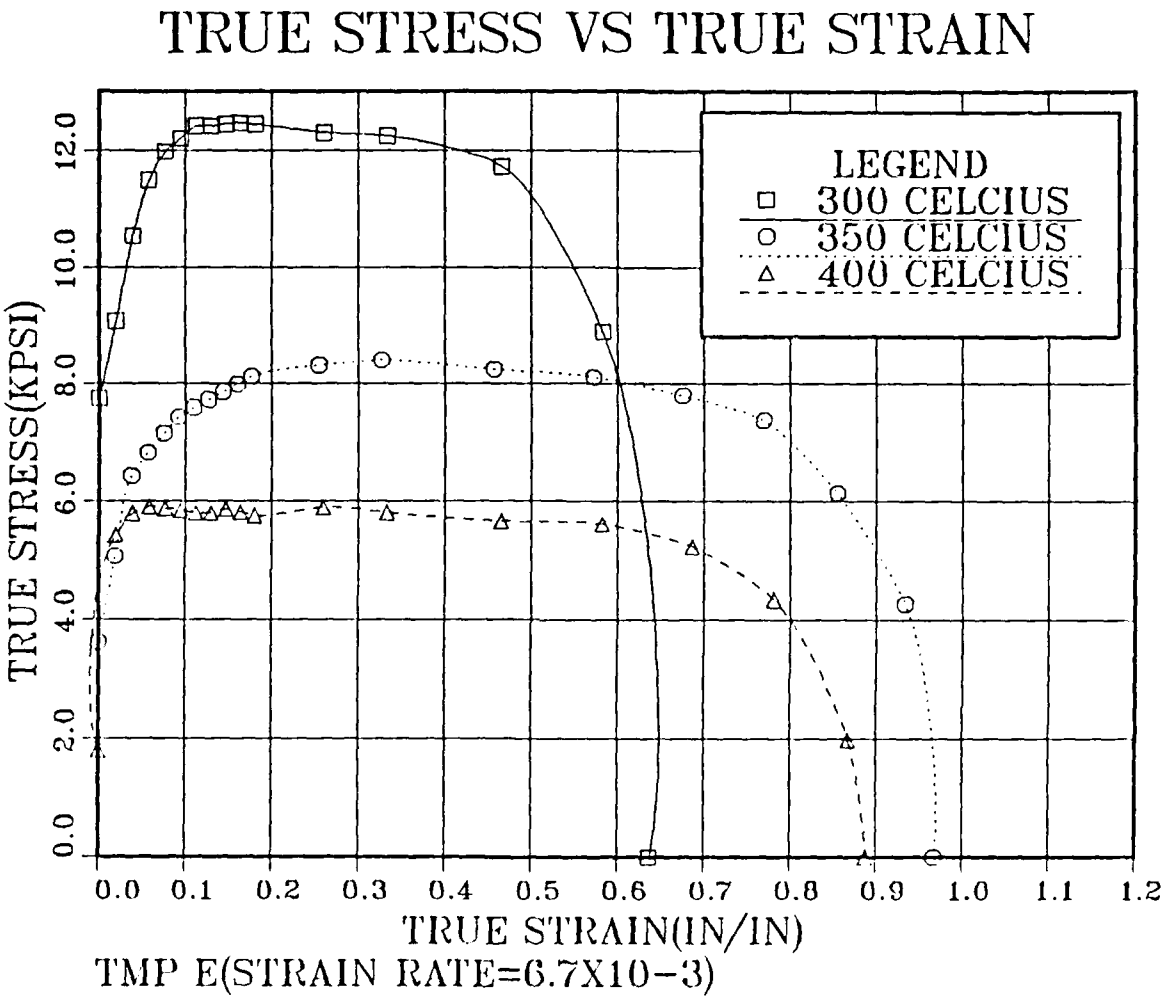

Figure 19. True Stress vs True Strain for material processed by TMP E: These data were obtained as a function of test temperature for strain rate of 6.7×10^{-3} s^{-1}.

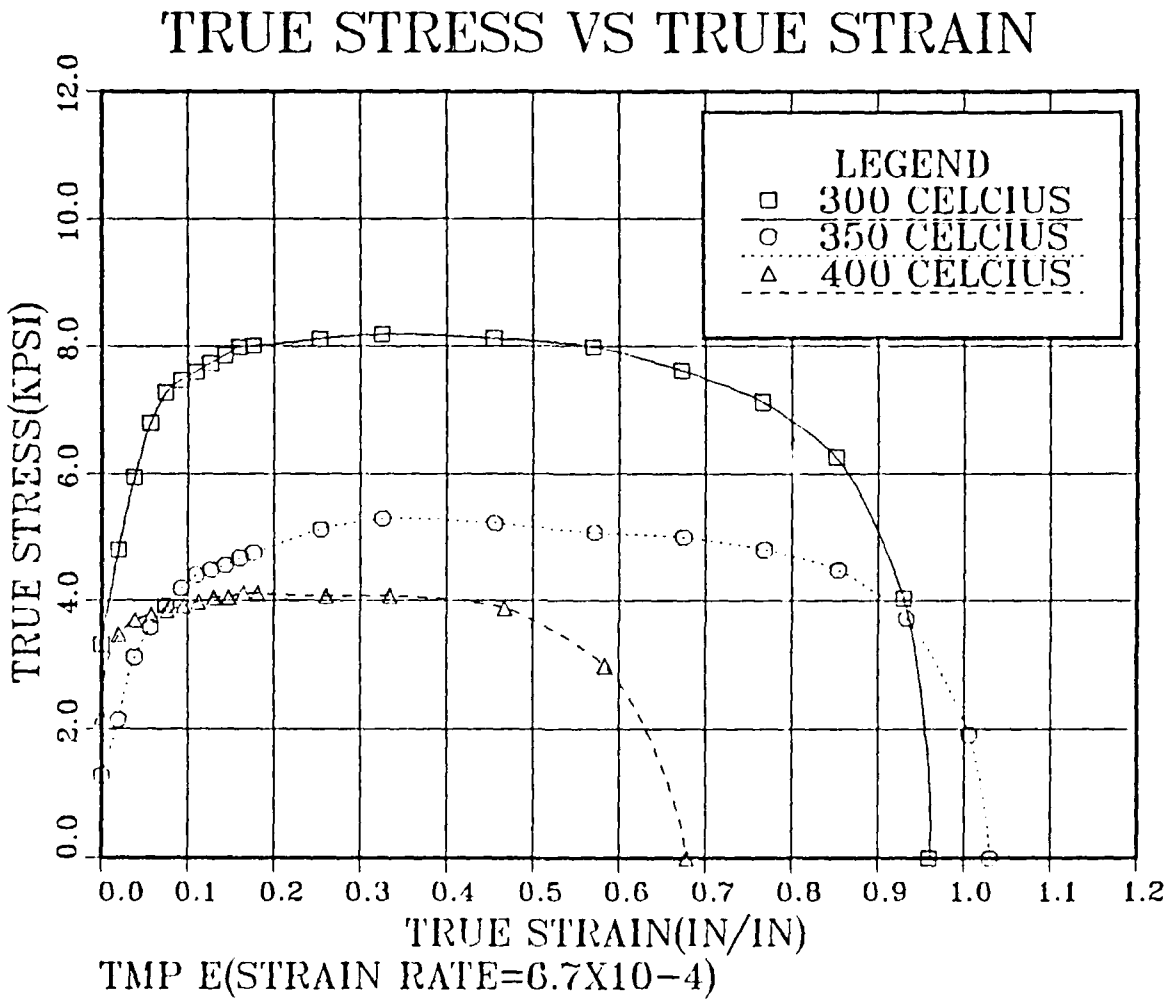

Figure 20. True Stress vs True Strain for material processed by TMP E: These data were obtained as a function of test temperature for strain rate of 6.7×10^{-4} s^{-1}.

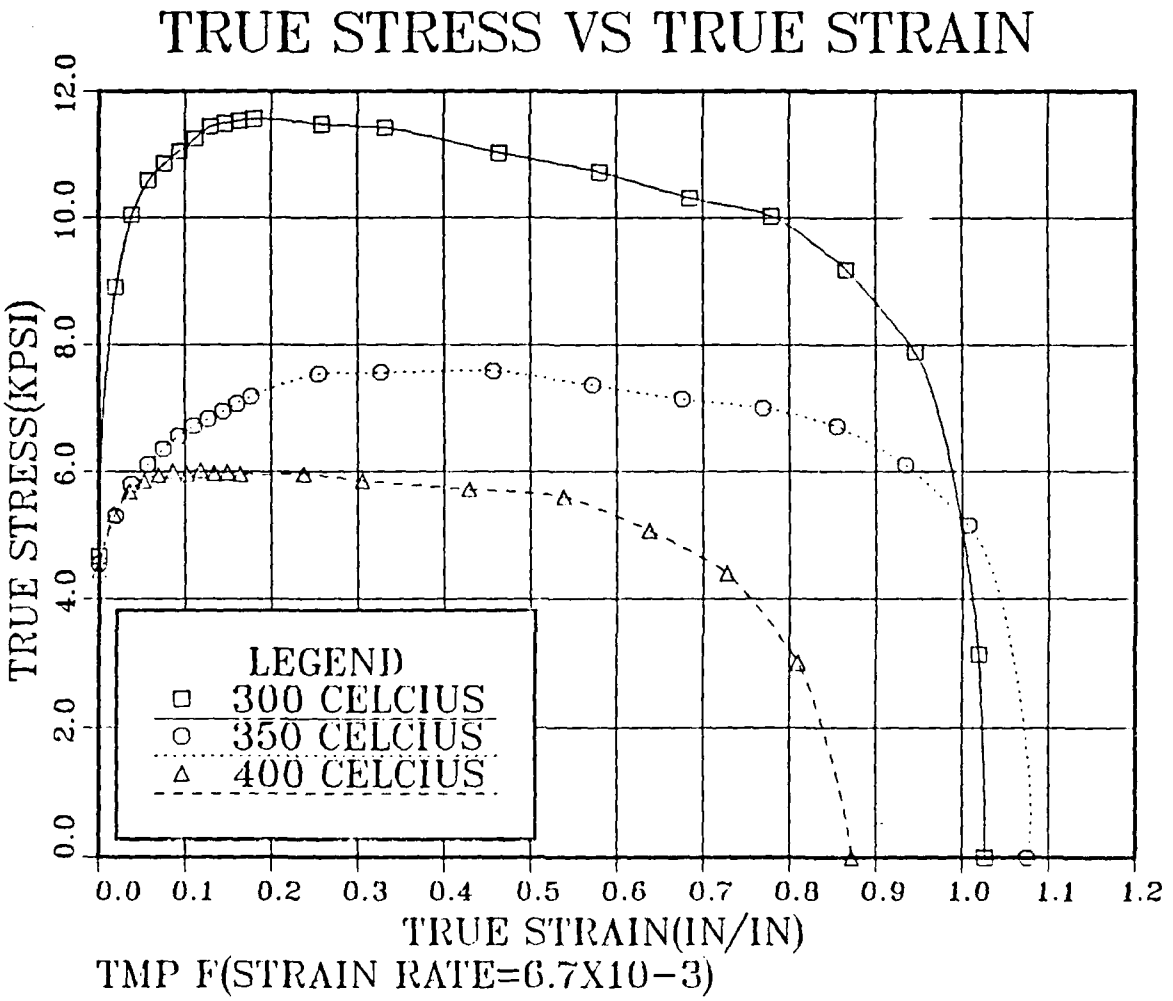

Figure 21. True Stress vs True Strain for material processed by TMP F: These data were obtained as a function of test temperature for strain rate of 6.7×10^{-3} s^{-1}.

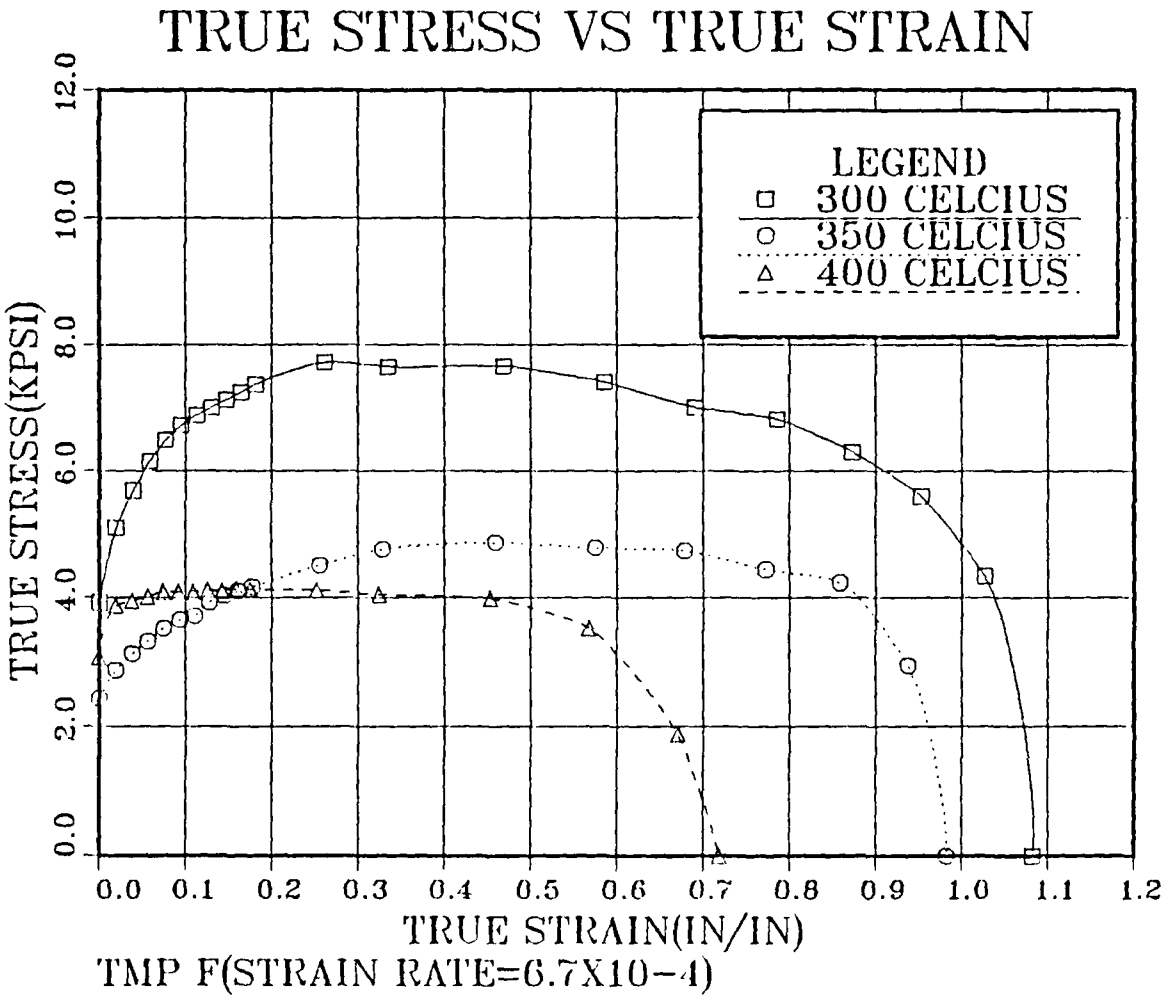

Figure 22. True Stress vs True Strain for material processed by TMP F: These data were obtained as a function of test temperature for strain rate of 6.7×10^{-4} s^{-1}.

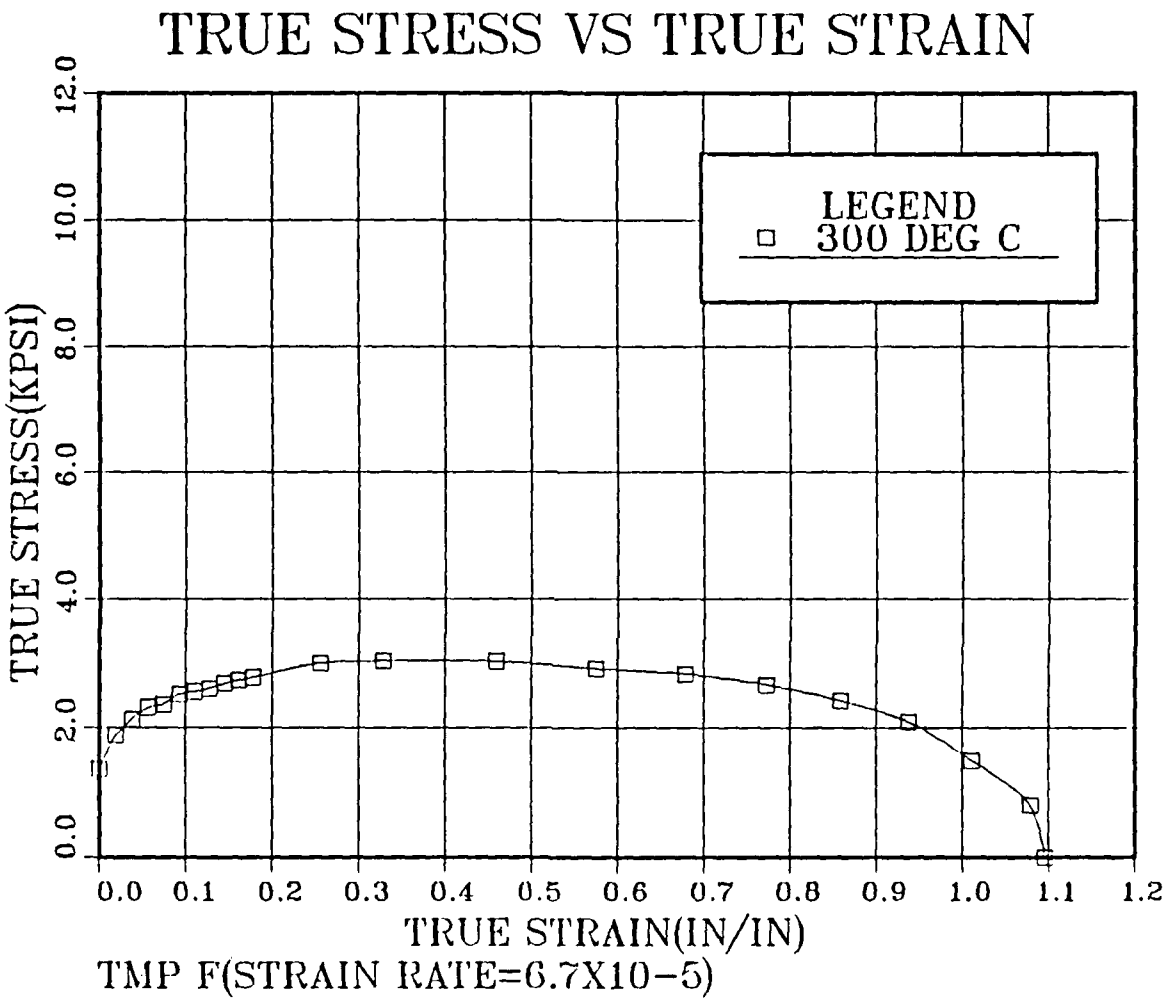

Figure 23. True Stress vs True Strain for material processed by TMP F: These data were obtained as a function of test temperature for strain rate of 6.7×10^{-5} s^{-1}.

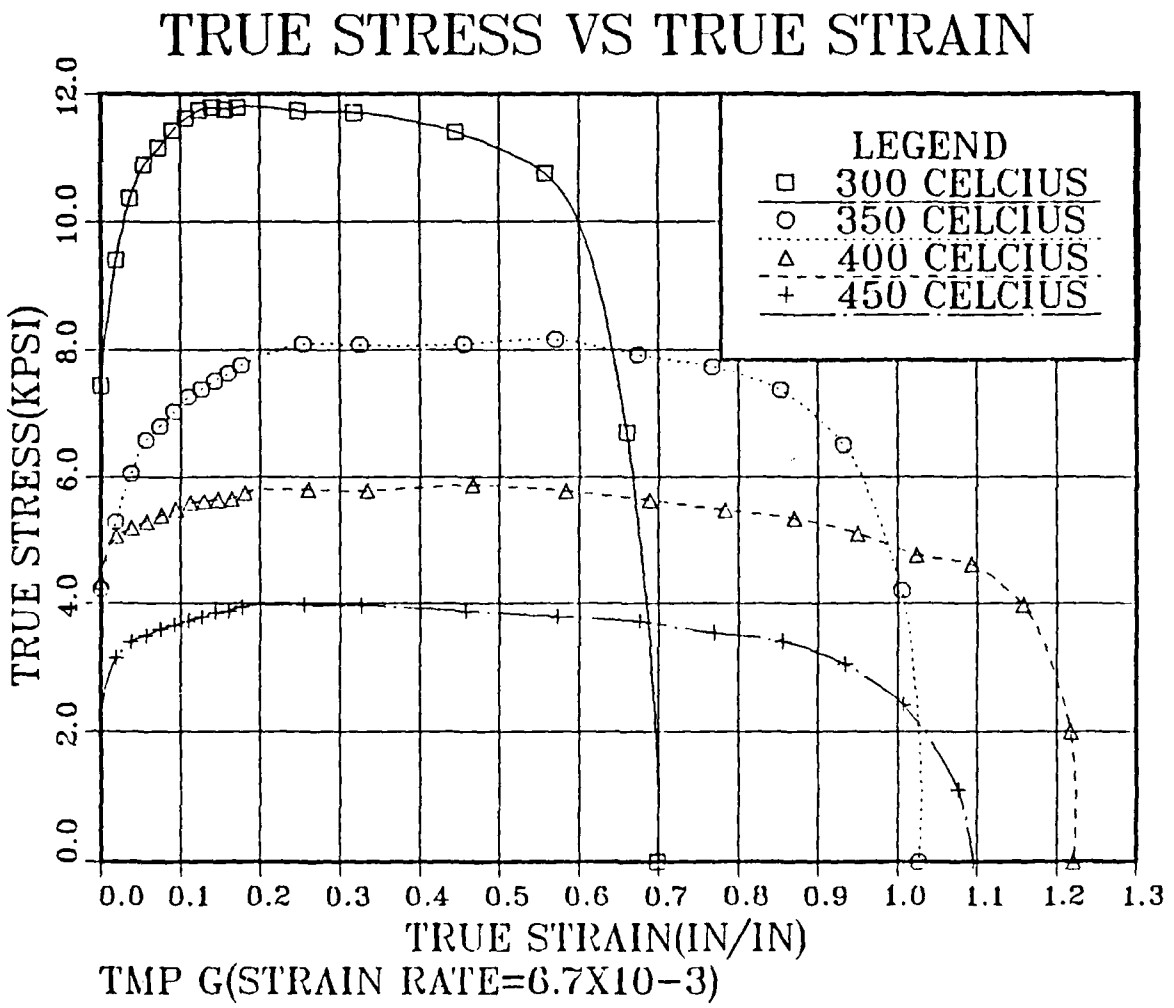

Figure 24. True Stress vs True Strain for material processed by TMP G: These data were obtained as a function of test temperature for strain rate of $6.7 \times 10^{-3}\ s^{-1}$.

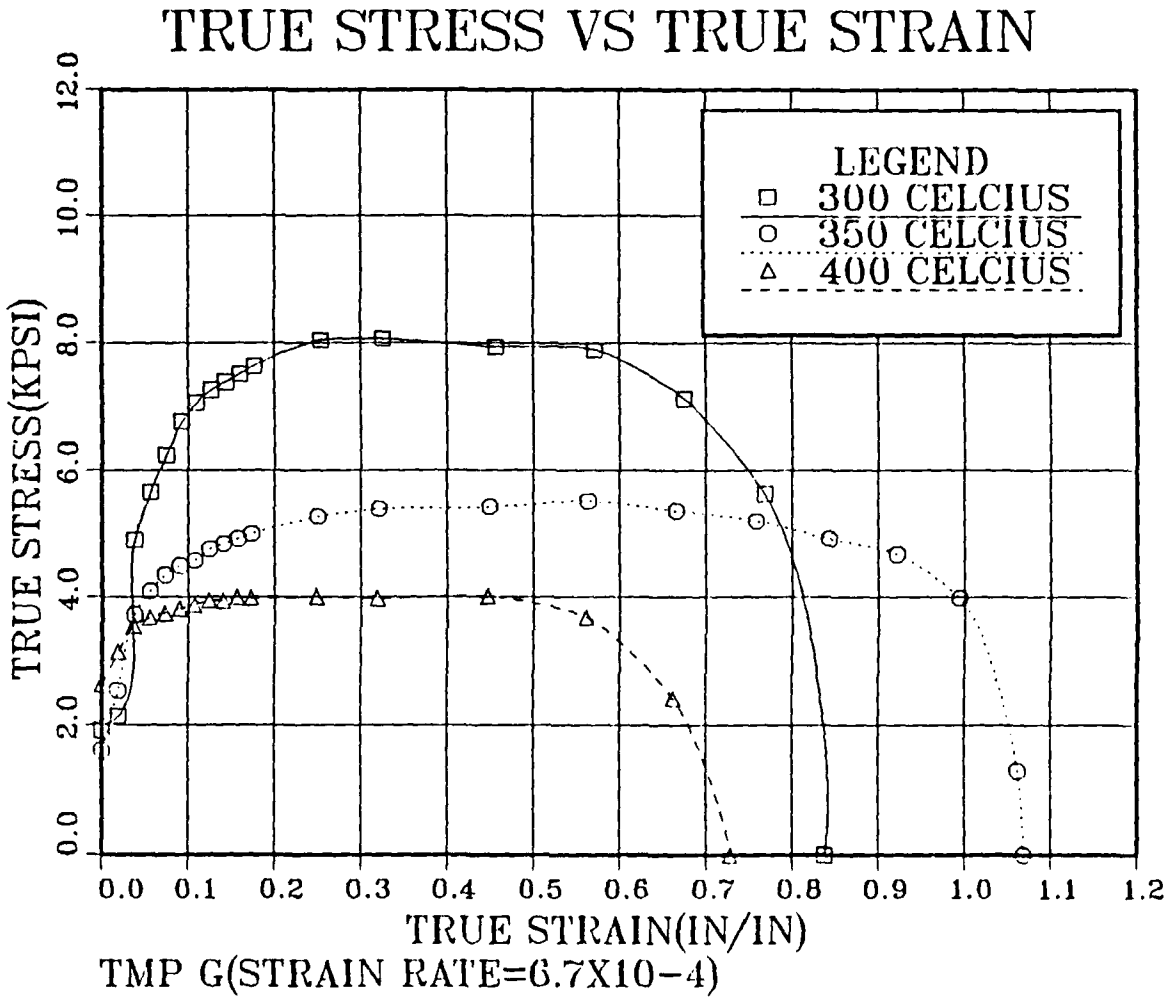

Figure 25. True Stress vs True Strain for material processed by TMP G: These data were obtained as a function of test temperature for strain rate of 6.7×10^{-4} s^{-1}.

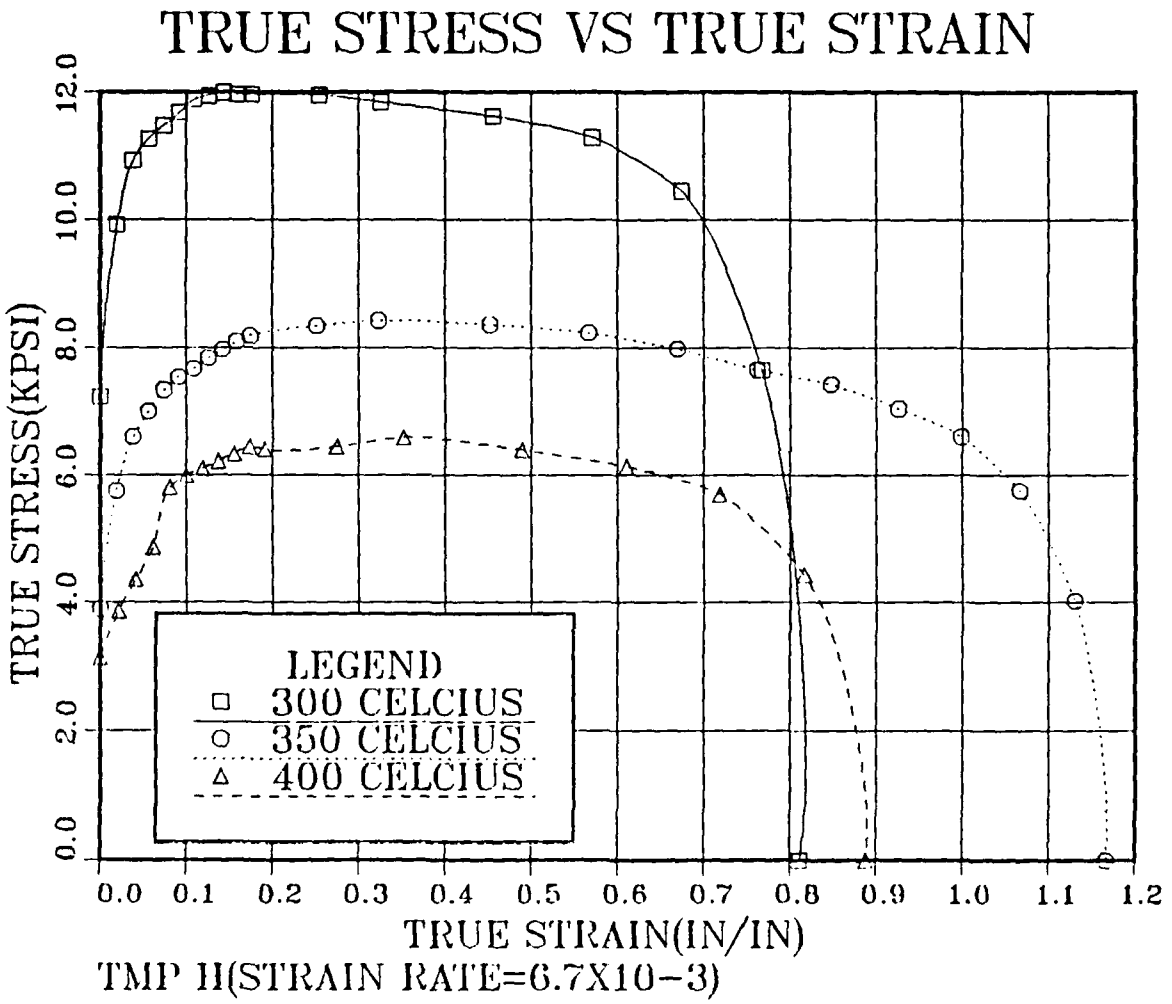

Figure 26. True Stress vs True Strain for material processed by TMP II: These data were obtained as a function of test temperature for strain rate of 6.7×10^{-3} s^{-1}.

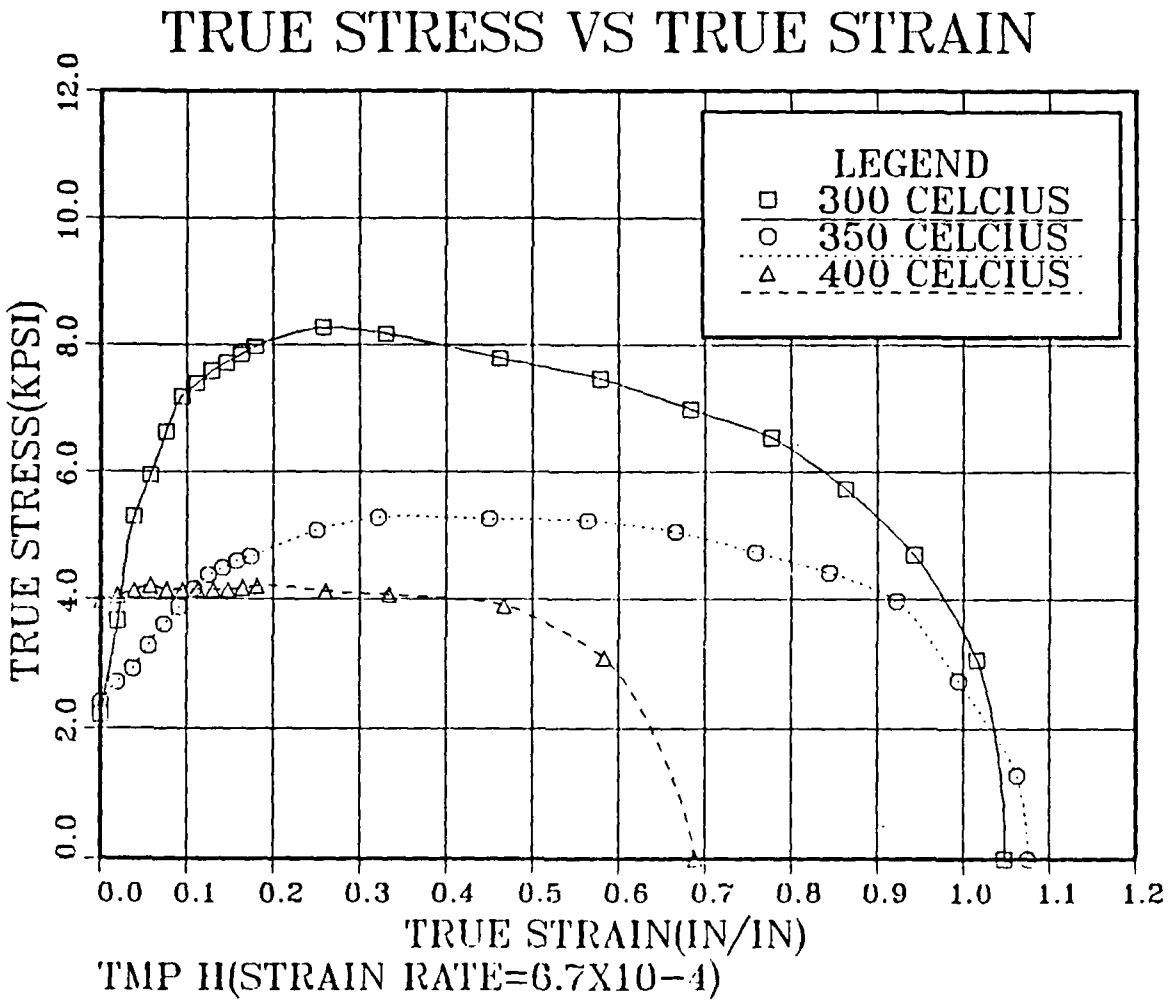

Figure 27. True Stress vs True Strain for material processed by TMP H: These data were obtained as a function of test temperature for strain rate of 6.7×10^{-4} s^{-1}.

APPENDIX B. PLOTS OF LOG STRESS VS LOG STRAIN RATE

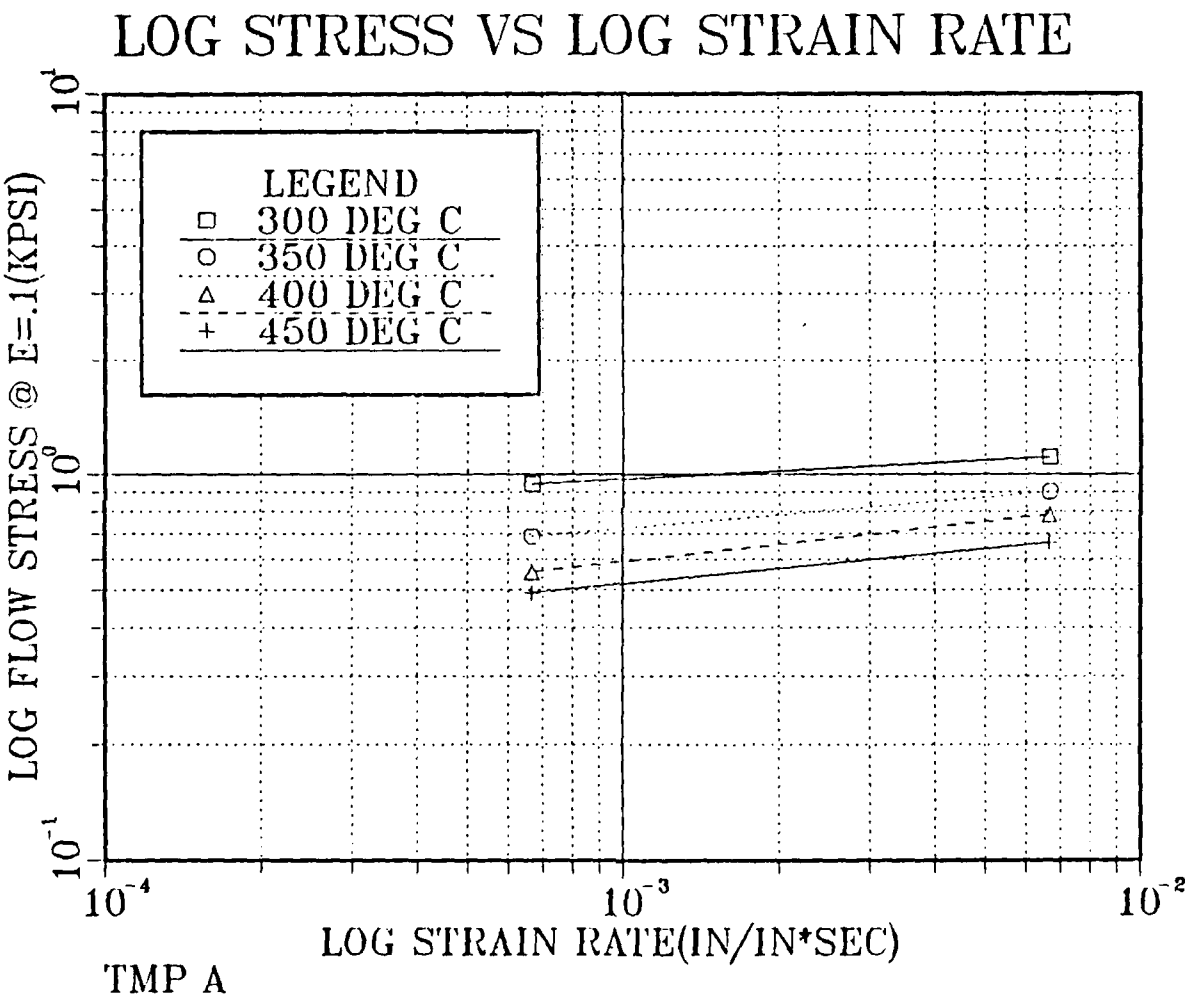

Figure 28. Log True Stress (at $\varepsilon = 0.1$) vs Log Strain Rate for TMP A.

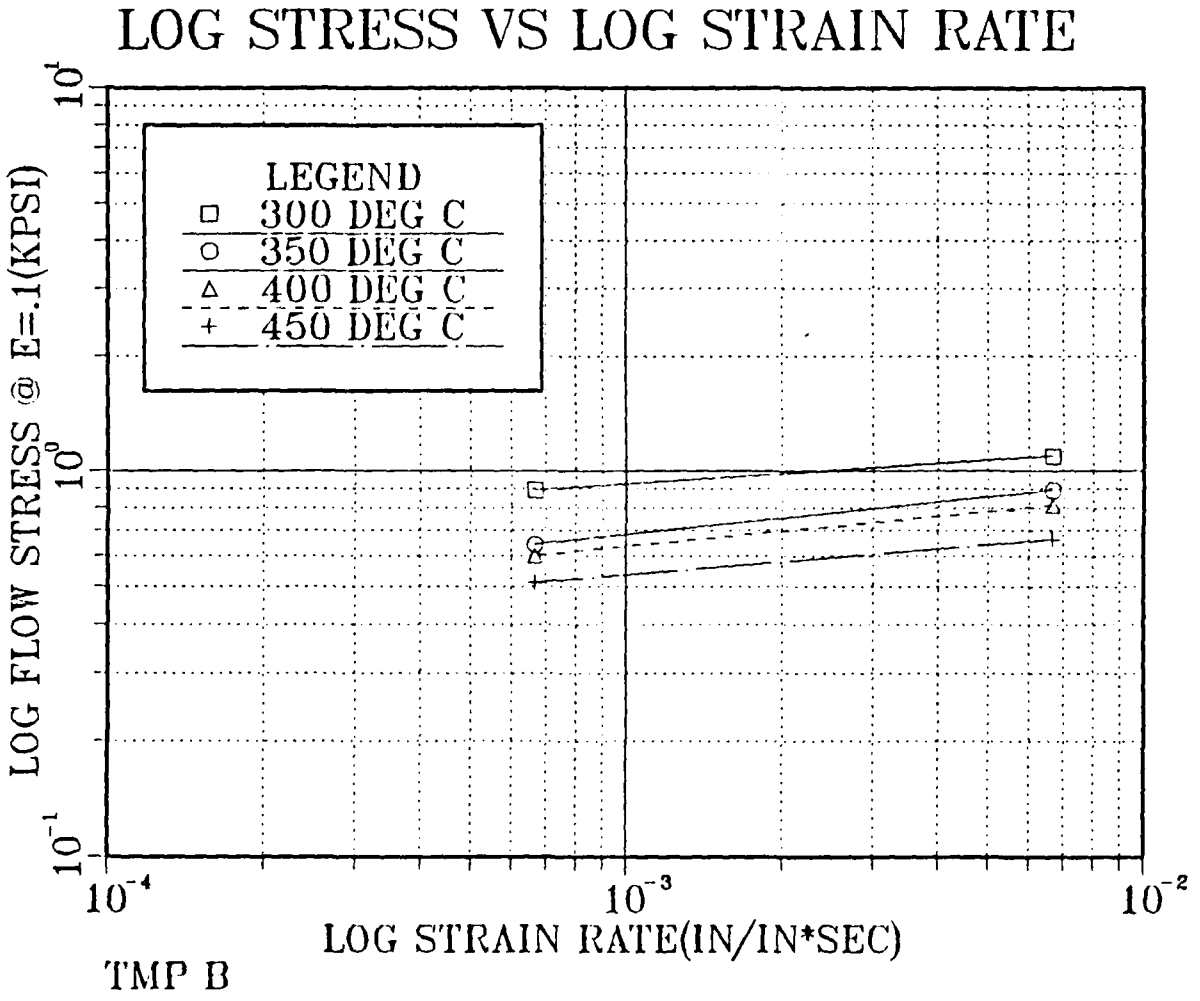

Figure 29. Log True Stress (at $\varepsilon = 0.1$) vs Log Strain Rate for TMP B.

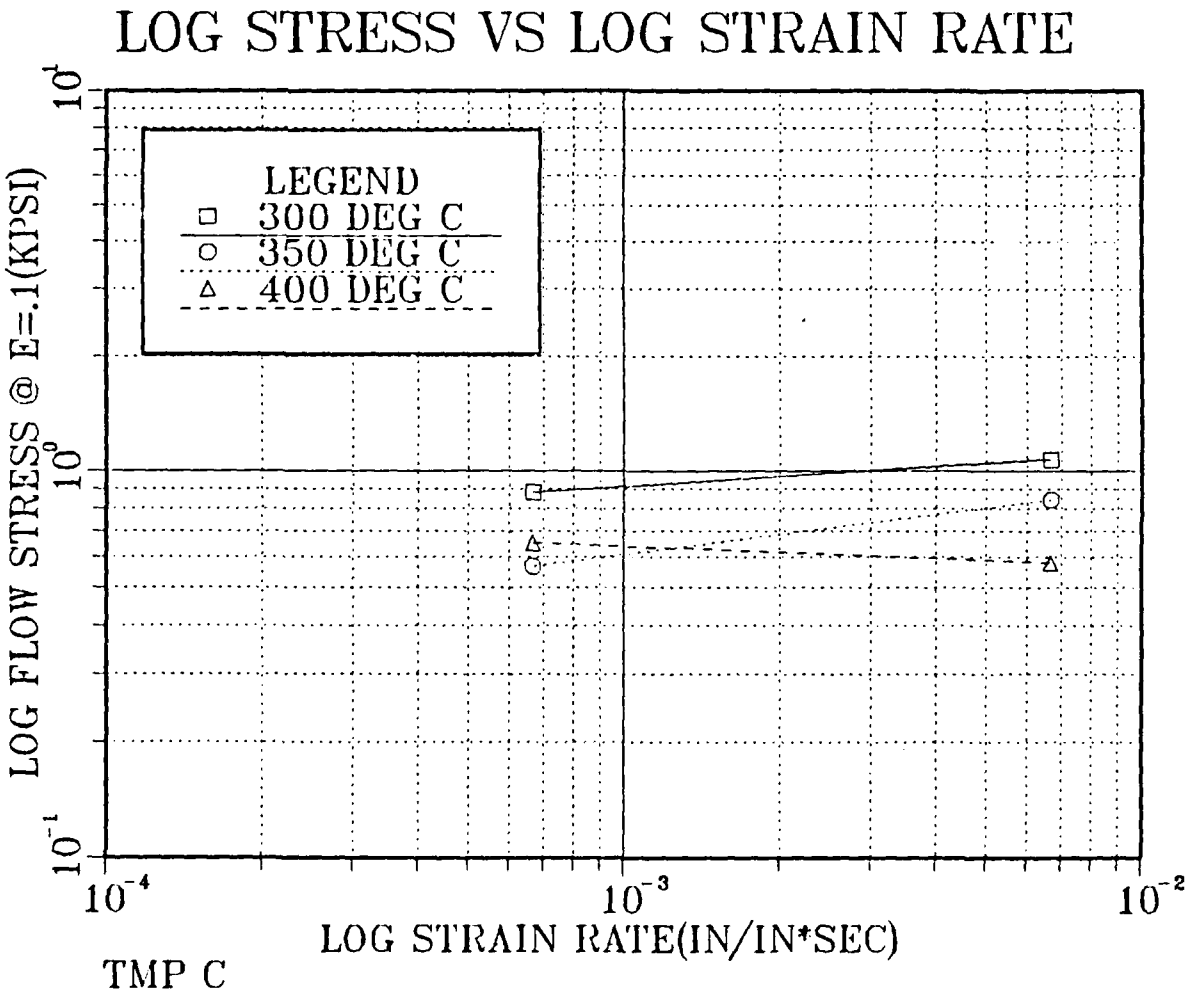

Figure 30. Log True Stress (at $\varepsilon = 0.1$) vs Log Strain Rate for TMP C.

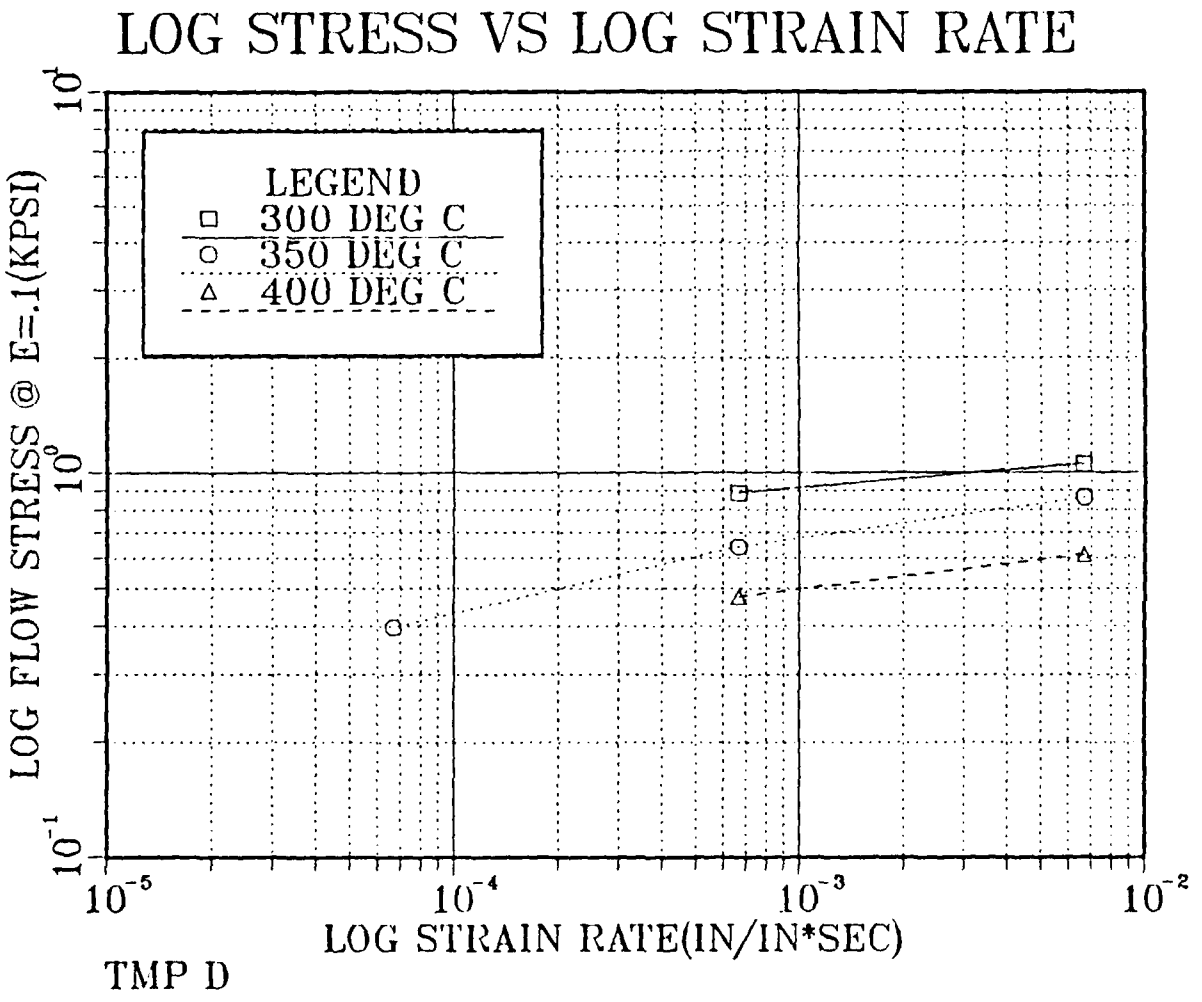

Figure 31. Log True Stress (at $\varepsilon = 0.1$) vs Log Strain Rate for TMP D.

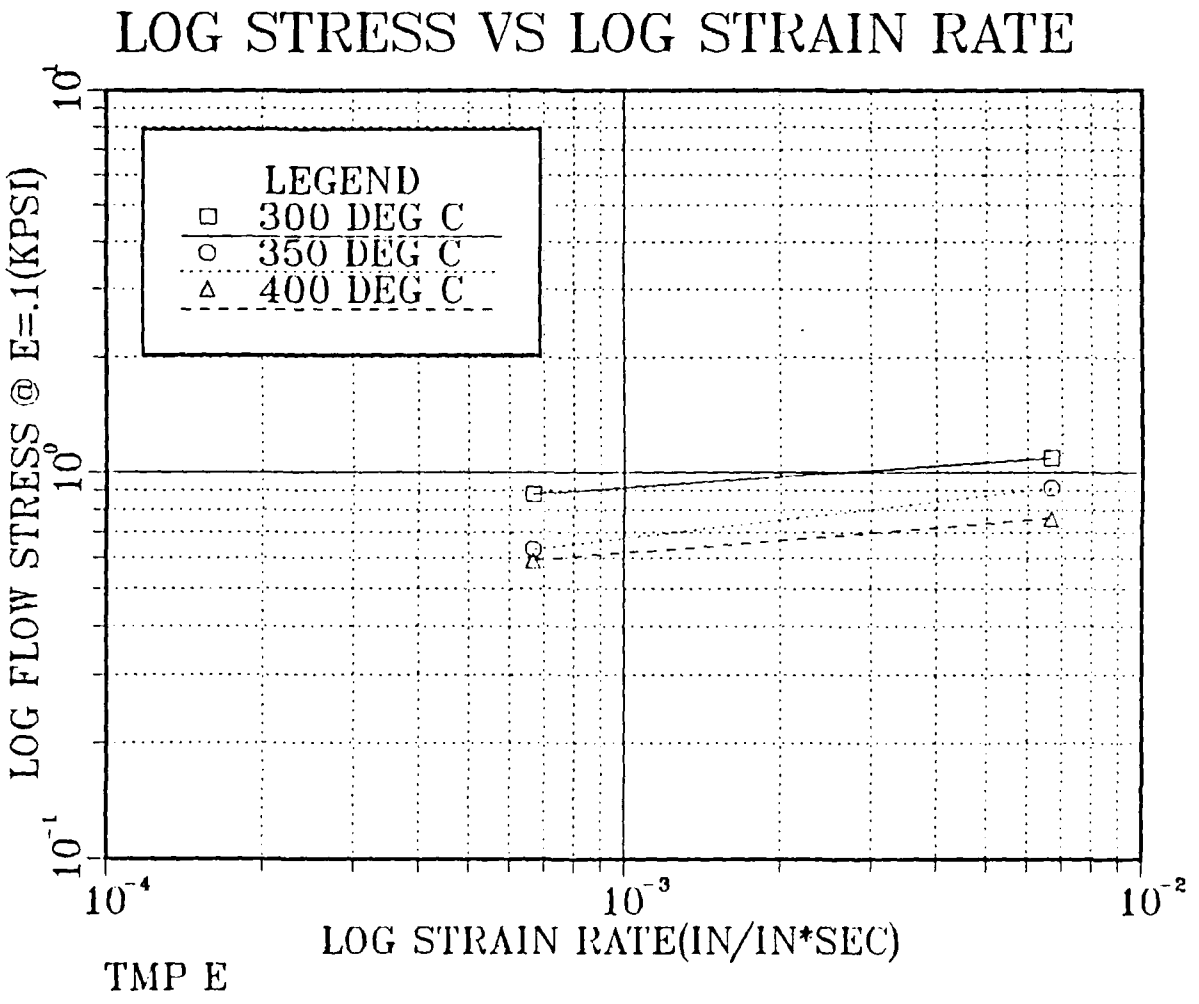

Figure 32. Log True Stress (at $\varepsilon = 0.1$) vs Log Strain Rate for TMP E.

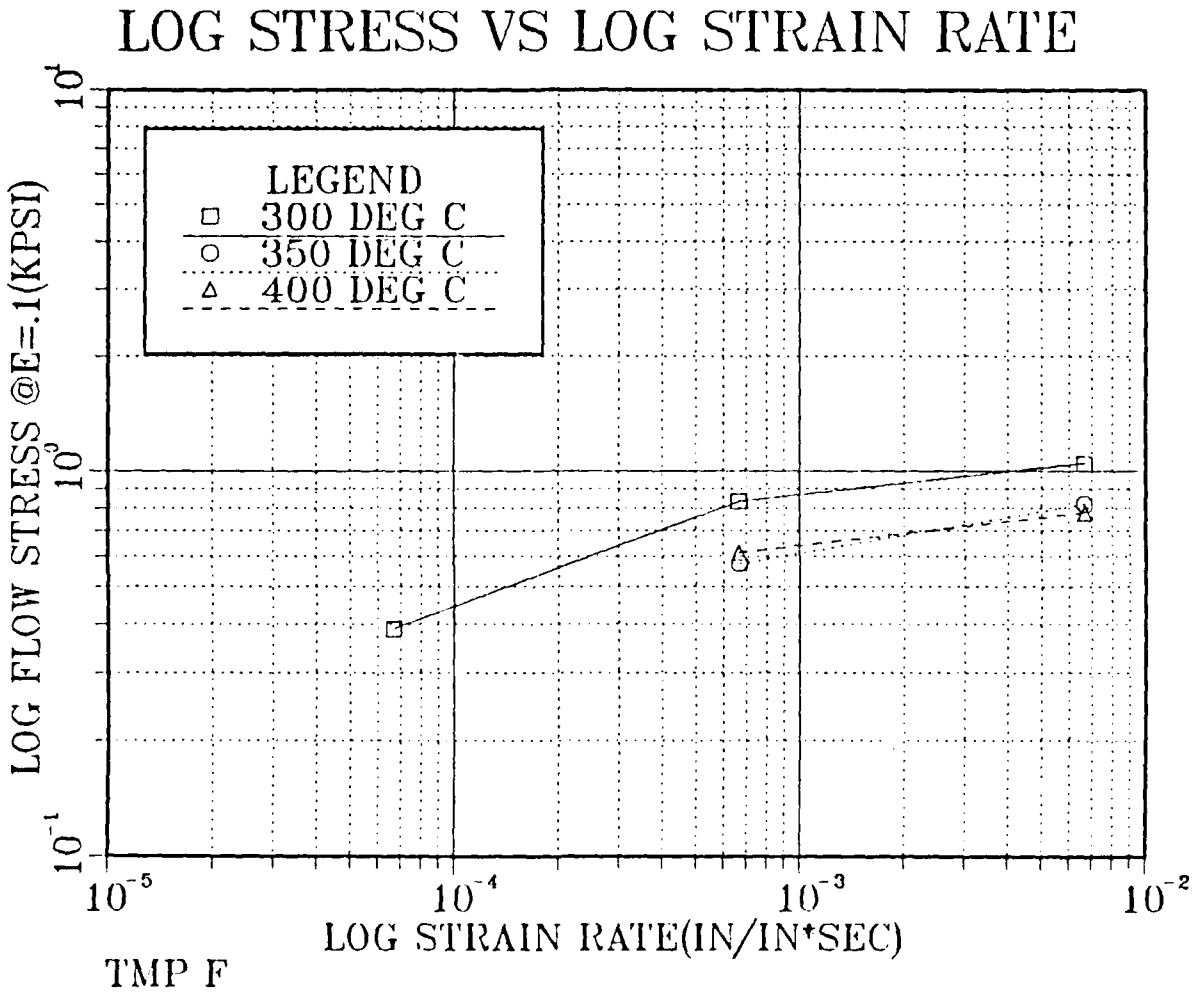

Figure 33. Log True Stress (at $\varepsilon = 0.1$) vs Log Strain Rate for TMP F.

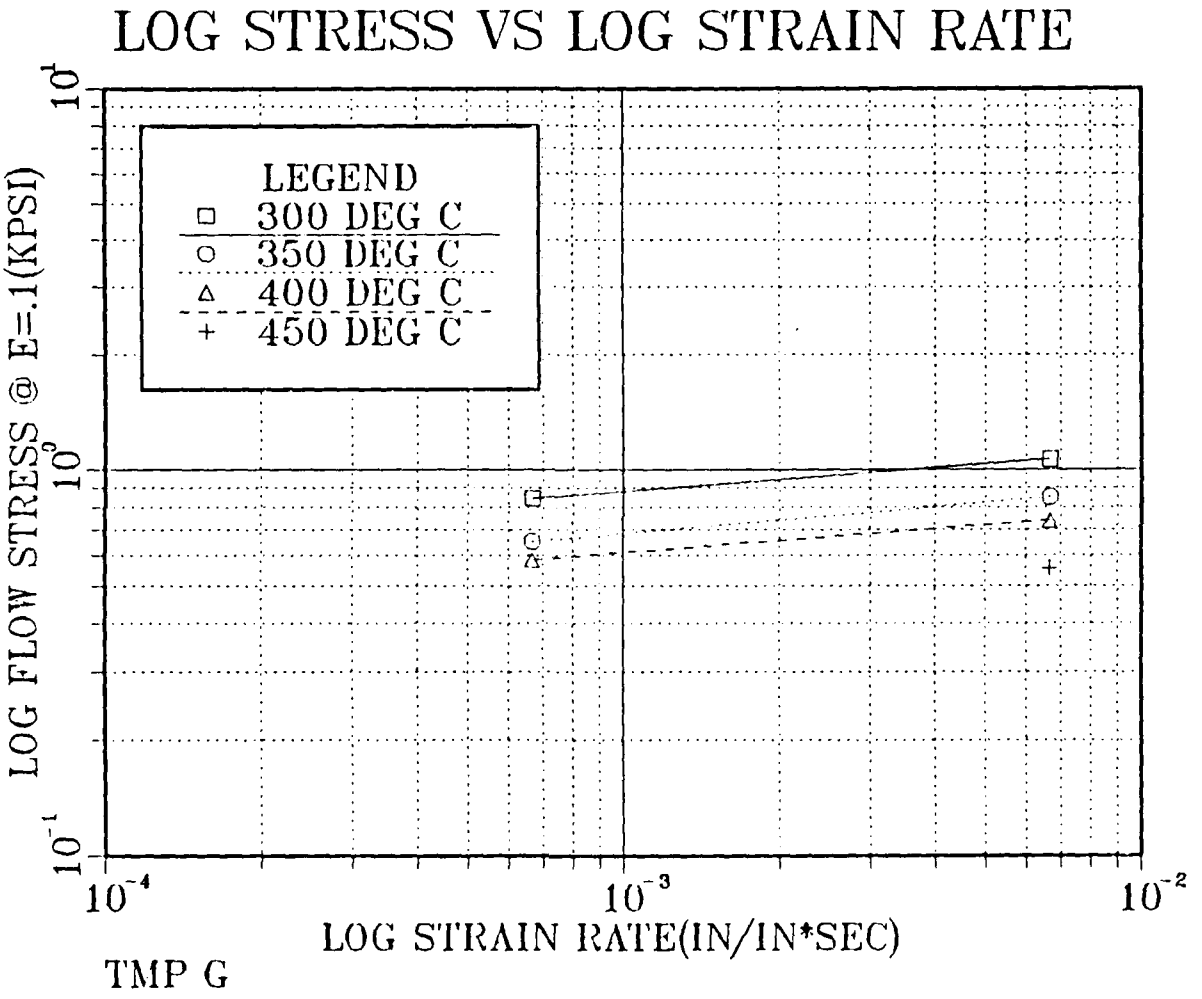

Figure 34. Log True Stress (at $\varepsilon = 0.1$) vs Log Strain Rate for TMP G.

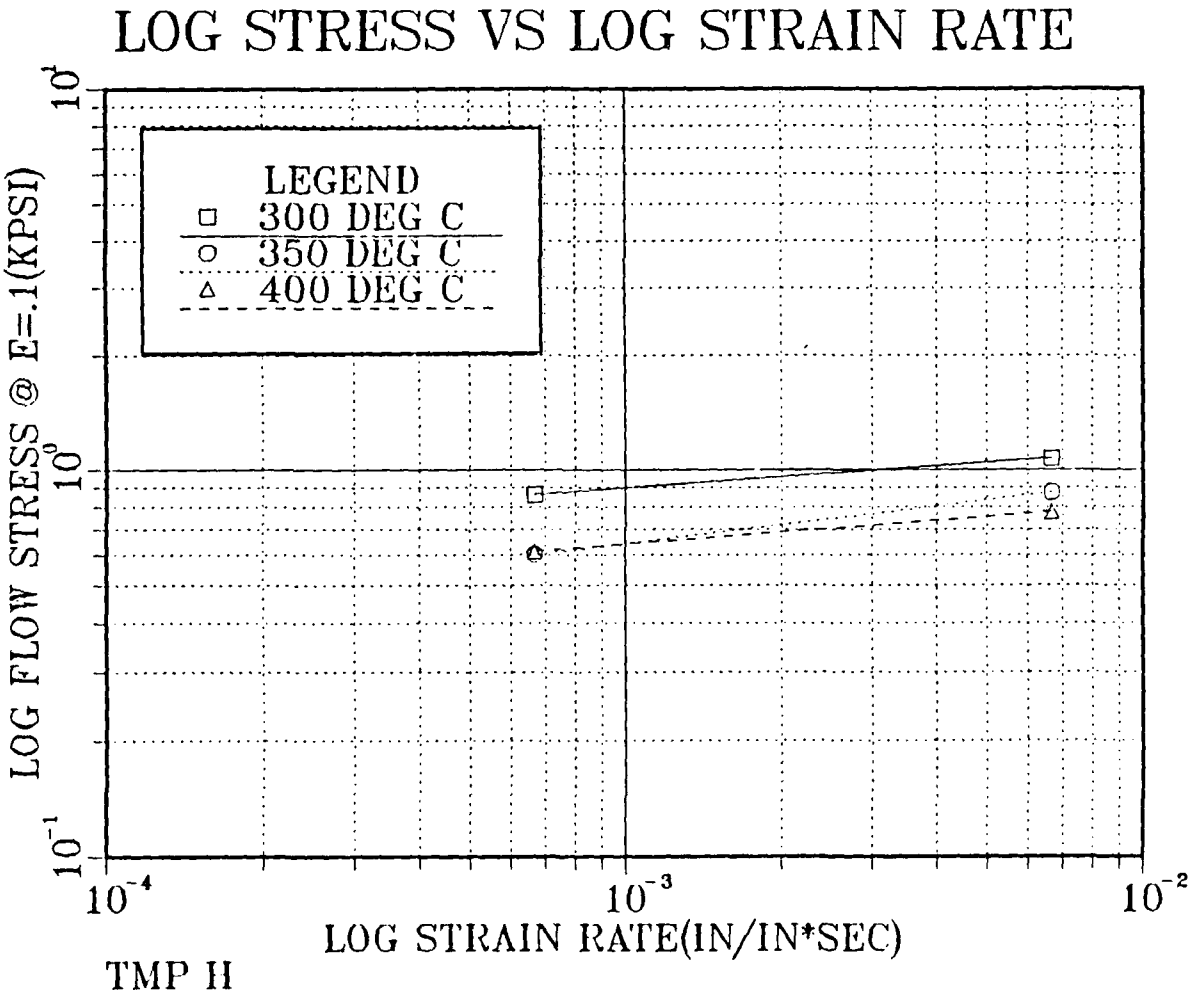

Figure 35. Log True Stress (at $\varepsilon = 0.1$) vs Log Strain Rate for TMP H.

LIST OF REFERENCES

1. Hales, S.J., and McNelley, T.R., "Fine-Grained Superplasticity at 300°C in a Wrought Al-Mg Alloy", *Superplasticity in Aerospace*, edited by Heikkenen, H.C., and McNelley, T.R., The Metallurgical Society, 1988.

2. Lee, E.-W., and McNelley, T.R., "Application of a Thermomechanical Process for the Grain Refinement of Aluminum Alloy 7475", *Materials Science and Engineering*, v.96, 1987.

3. Kobayashi, M., "Novel Processing Methods for Superplastic Alloys", *Superplasticity and Superplastic Forming*, edited by Hamilton, C.H., and Paton, N.E., The Minerals, Metals & Materials Society, 1988.

4. Wert, J.A., "Grain Refinement and Grain Size Control in Superplastic Forming", *Journal of Metals*, September 1982.

5. *Aluminum Properties and Physical Metallurgy*, edited by Hatch, J.E., American Society for Metals, 1984.

6. Private communication between Staley, J.T., Alcoa Technical Center, Alcoa Center, PA, and McNelley, T.R., September 1986.

7. *Metals Handbook*, 9th ed., v.4, American Society for Metals, 1981.

8. Anamet Laboratories, Inc., Laboratory Number: 589.042 to Naval Postgraduate School, Subject: Chemical Analysis of Al 7475, 18 May 1989.

9. Groh, G.E., *Processing of Aluminum Alloy 2090 for Superplasticity*, Master's Thesis, Naval Postgraduate School, Monterey, CA, September 1988.

10. *Metals Handbook*, 9th ed., v.9, American Society for Metals, 1985.

INITIAL DISTRIBUTION LIST

		No. Copies
1.	Defense Technical Information Center Cameron Station Alexandria, VA 22304-6145	2
2.	Library, Code 0142 Naval Postgraduate School Monterey, CA 93943-5002	2
3.	Department Chairman, Code 69Hy Department of Mechanical Engineering Naval Postgraduate School Monterey, CA 93943	1
4.	Naval Engineering Curricular Office, Code 34 Naval Postgraduate School Monterey, CA 93943	1
5.	Professor T.R. McNelley, Code 69Mc Department of Mechanical Engineering Naval Postgraduate School Monterey, CA 93943	5
6.	Naval Air Systems Command, Code AIR931 Naval Air Systems Command Headquarters Washington, DC 20361	1
7.	Director Naval Research Lab Washington, DC 20375	1
8.	LT John Ratkovich 1555 Ashcroft Way Sunnyvale, CA 94087	2